Materials Science & Engineering R 163 (2025) 100934

Contents lists available at ScienceDirect

Materials Science & Engineering R

journal homepage: www.elsevier.com/locate/mser

All-in-one self-powered wearable biosensors systems

Qianying Li [a,b], Mingyuan Gao [c], Xueqian Sun [a], Xiaolin Wang [a], Dewei Chu [d], Wenlong Cheng [e], Yi Xi [b,*], Yuerui Lu [a,*]

[a] School of Engineering, Computing & Cybernetics, Australian National University, Canberra, ACT 2602, Australia
[b] Department of Applied Physics, School of Physics, Chongqing University, Chongqing 400044, PR China
[c] College of Engineering and Technology, Southwest University, Chongqing 400716, PR China
[d] School of Materials Science and Engineering, University of New South Wales, Sydney, NSW 2052, Australia
[e] School of Biomedical Engineering, Faculty of Engineering, The University of Sydney, NSW 2008, Australia

ARTICLE INFO

Keywords:
Wearable biosensors
Self-powered technologies
All-in-one engineering
Material engineering
Energy management

ABSTRACT

Wearable biosensors capable of long-term operation facilitate future precision medicine and personalized health monitoring by in-situ acquisition, real-time processing, and continuous transmission of biological signals. Self-powered technologies provide effective strategies to achieve the above goals, but make the entire bioelectronic system more complex. Ultimately, challenges of material engineering, miniaturization, and performance enhancement converge into the all-in-one engineering of self-powered wearable biosensor systems. Matching the power output of the energy module with the power consumption requirements of the signal module is the basic prerequisite for achieving all-in-one design. This review takes power as the entry point to comprehensively analyze and summarize the mechanisms, performance ranges, enhancement strategies, application examples, and future prospects of self-powered wearable biosensors. We review the principles, engineering strategies, and capabilities in energy collection, management, and storage of current self-powered technologies to determine the output power range and methods for performance enhancement. Next, we discuss and compare the strategies and mechanisms for signal acquisition, processing, and transmission, focusing on the performance, size, wearability and enhancement strategies of each module. Most importantly, we summarize the four representative all-in-one engineering strategies in the system, covering design principles, basic materials, targeted parts, integration levels, advantages and disadvantages. Finally, we outline key challenges and potential solutions for six modules in preparation for intelligent and networked sensing.

1. Introduction

A biosensor is a self-contained, integrated analytical device that comprises a recognition element based on biologically sensitive materials, along with the appropriate physicochemical transducer and the signal processor [1]. It converts rich biological information from the surrounding environment, body surface, and internal body into measurable electrical signals. Since the successful development of the glucose enzyme electrode in 1962 brought the concept of biosensors to the public [2], the signal sources of biosensors have expanded from common vital signs and body movements to bodily fluids such as blood, sweat, and tears [3]. Combined with wearable technologies, wearable biosensors have emerged as an extension of traditional biosensors. They enable continuous and convenient monitoring of biological signals in a non-invasive or minimally invasive manner. Moreover, advancements in flexible materials, stretchable circuit design, and advanced manufacturing techniques, have transformed wearable biosensors from bulky first-generation medical devices into lightweight, miniature bioelectronic devices, paving the way for truly personalized healthcare [3,4]. For example, the evolution from first-generation washable glucometers to current continuous glucose monitoring systems, and even blood glucose monitors, has shifted the monitoring of blood glucose levels from hospital settings to personal homes and workplaces [5]. Therefore, current wearable biosensors are evolving towards miniaturization, intelligence, multifunctionality, and networking [6].

Most wearable biosensors can be disassembled into four main parts: energy source, signal collecting component, signal processing component and signal transmission component. Among these components, the typical energy source is a commercial battery, which remains the most challenging part to miniaturize and make flexible [6]. Encouragingly,

* Corresponding authors.
E-mail addresses: yxi6@cqu.edu.cn (Y. Xi), yuerui.lu@anu.edu.au (Y. Lu).

https://doi.org/10.1016/j.mser.2025.100934
Received 7 November 2024; Received in revised form 25 December 2024; Accepted 15 January 2025
Available online 8 February 2025

the natural environment and human body contain abundant energy, including light energy, mechanical energy, thermal energy, bioenergy, moisture energy, etc. Flexible and lightweight self-powered technology can convert the above energy into usable electrical energy based on various physical effects such as the photovoltaic effect, triboelectric effect, thermoelectric effect, etc [7]. Based on built-in switching and triboelectric nanogenerator (TENG) technology, an active sensor achieves peak power in the watt range [8]. Additionally, wireless power transfer (WPT) technology can deliver electrical energy to a magneto-electric material less than one square centimeter through one-centimeter-thick biological tissue, with a power density exceeding 200 milliwatts per square centimeter [9], demonstrating the potential to power higher-consumption bioelectronics. By adopting self-powered technologies, wearable biosensor systems obtain continuous power supply while minimizing the area occupied by energy storage devices, thereby ensuring a long lifetime and safety. For example, organic pulse oximeters integrated with amorphous silicon solar cells (SCs) can enable continuous, self-powered pulse oximetry measurements [10,11]. Furthermore, self-powered signal acquisition modules have further enriched wearable biosensor systems, leading to the development of active sensors. By actively capturing the voltage changes in triboelectric materials caused by blinking, a self-powered mechnosensational communication system realizes real-time human-machine interface operations such as smart home control and wireless hands-free typing [12]. Therefore, the self-powered wearable biosensor system module mainly focuses on energy supply and sensing, which is divided into six major modules: energy collection, management and storage, and signal acquisition, processing and transmission.

The ideal all-in-one wearable biosensors collect energy from the natural environment and the human body to supply their energy consumption (Fig. 1**A**). In this review, we summarize and analyze the performance and size data of more than 200 self-powered wearable biosensors (Fig. 1**B**), intuitively demonstrating the integration level of the self-powered wearable biosensor and the synergy effect between various modules. Fig. 1**C** briefly shows the writing logic of the main content of this review. Firstly, we discuss eight energy harvesting technologies with self-powered property, focusing on the mechanism, sizes, output power, and performance improvement strategies. Then, we summarize the energy management and storage strategies along with their performance (power consumption, conversion efficiency), analyzing the underlying principles and potential areas for improvement. In the sensing section, wearable biosensors consist of commercial products and emerging active sensors. Since commercial wearable biosensors integrate signal acquisition, processing and transmission, their power consumption is more worthy of discussion. For active sensors, the signal source, sensing principles, and improvements in sensitivity are particularly worth discussing. Importantly, we summarize and analyze four all-in-one engineering technologies that are crucial for self-powered wearable biosensors, covering mechanism, base materials, targeted parts, degree of integration, advantages and disadvantages. Then, four main signal transmission technologies are discussed in terms of energy consumption, transmission distance, etc. Furthermore, four examples of fully all-in-one representative self-powered wearable biosensor systems are presented, covering wireless e-health patches, implantable

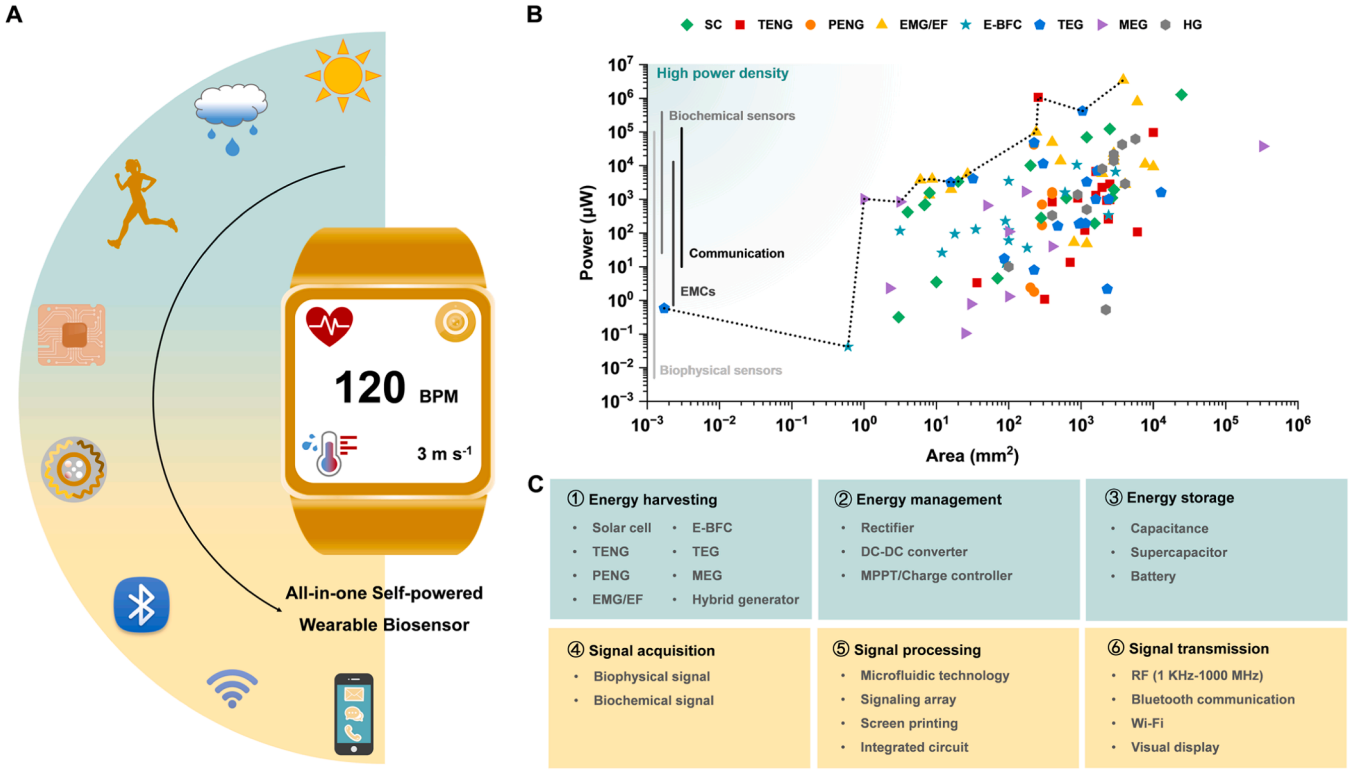

Fig. 1. Rationale for the system of all-in-one self-powered wearable biosensors. (A) Schematic illustration of the all-in-one self-powered wearable biosensor. (B) Comparing the power densities of self-powered technologies. Self-powered technologies include solar cell (SC), triboelectric nanogenerator (TENG), piezoelectric nanogenerator (PENG), electromagnetic generator (EMG)/ wireless power transmission technology based on electromagnetic field (EF), enzyme-based biofuel cells (E-BFC), thermoelectric generator (TEG), moisture-electric generator (MEG), and hybrid generators (HG). Based on the literature statistics, an envelope (dashed line) is constructed by joining the self-powered technologies with the highest power within a given effective area from left to right. The highest point of the envelope is the device that generates the highest power among all the self-powered technologies counted. All self-powered technologies located on the envelope line have the highest output power within the effective area, which means they have the maximum power density. The four vertical lines near the y-axis represent the power ranges required by common biosensors, energy management circuits (EMCs) and communication technologies. (C) A step-by-step design process for the all-in-one wearable biosensor from energy and signal perspectives, including (1) energy harvesting, (2) energy management, (3) energy storage, (4) signal collection, (5) signal processing, and (6) signal transmission. MPPT, the maximum power point tracker. RF, radio frequency. Wi-Fi, Wireless Fidelity.

biosensing devices, and smart e-textiles. Finally, we discuss the current challenges faced by each of the six modules and make recommendations, taking smart contact lenses as an example to look into the future prospects of biosensors.

2. Self-powered technologies support all-in-one wearable biosensor systems

To convert the scattered energy into electrical energy, three components are required: energy harvesting, energy management and energy storage. These three components are collectively referred to as self-powered technologies, which support the integration of wearable biosensor systems. Energy harvesters are divided into eight categories, including SC, TENG, piezoelectric nanogenerator (PENG), electromagnetic generator (EMG)/wireless power transmission technology based on electromagnetic field (WPT-EF), enzyme-based biofuel cell (E-BFC), thermoelectric generator (TEG), moisture-electric generator (MEG), and hybrid generators (HGs). Fig. 1**B** and Table S1 systematically display the effective area and output power of various energy harvesters. A black dashed envelope is constructed in Fig. 1**B** by connecting the energy harvesters with the highest power output within a given active area. The black dashed envelope compares the performance of the energy harvesters in terms of effective area and output power, and also vividly represents the highest power density of the energy harvesters currently used to power wearable biosensors. Moreover, the power consumption ranges of various biosensors, energy management circuits (EMCs) and communication technologies are shown as three vertical lines near the y-axis. Next, from the perspective of energy, this section provides an in-depth analysis of eight types of energy harvesters and their commonly used energy management and energy storage units, along with the mechanisms, key influencing factors, performance, enhancement strategies and limitations. The black dashed envelope and the three vertical energy consumption lines near the y-axis are retained in the performance statistics graphs of various energy harvesters for further analysis.

2.1. Solar cells

The solar radiation intensity above the Earth's atmosphere is about 1357 W m^{-2} (solar constant), of which about 50 % can reach the ground through the atmosphere [13]. Therefore, the large amount of solar energy in the natural environment provides the basis for realizing self-powered wearable sensors. In 1883, Charles Fritz invented the first SC based on the phenomenon of photoconductivity by coating a very thin layer of Au with selenium, which had an energy conversion efficiency of 1 %. Modern SCs were first invented by scientists at Bell Laboratories in 1954 [14]. These primitive SCs initially had an efficiency of about 6 %. The larger band gap of AlGaAs (1.42–2.16 eV) has increased the efficiency of solar cells based on this material to 20 % [15]. Based on the photoelectric effect, when photons are injected into the semiconductor, electron-hole pairs are excited in the PN junction area [16]. Under the action of the built-in electric field, electrons migrate toward the N-type semiconductor and holes migrate toward the P-type semiconductor [17]. After connecting the back electrodes of the semiconductor, the current is generated in the external circuit (Fig. 2**A**). So far, SCs can be divided into three generations. As the first-generation photovoltaic technology, silicon-based solar cell technology dominates

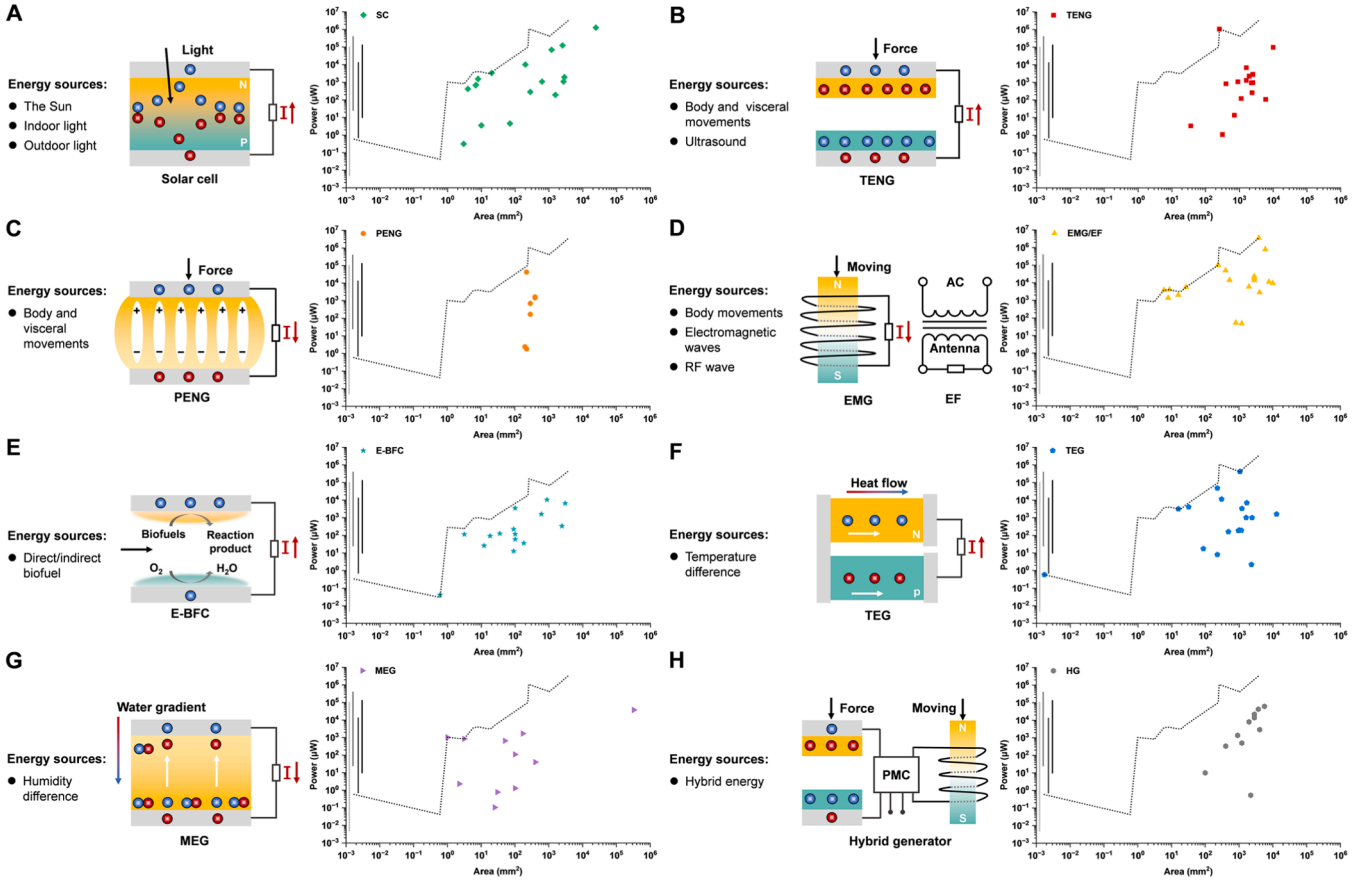

Fig. 2. Working mechanism and power density of self-powered technologies. In the power diagrams of Fig. 2, the envelope of the highest power within the given effective area for the self-powered technology (the black dashed line) is retained. This is to highlight the differences between this self-powered technology and the current state-of-the-art. The power ranges of the biosensors, EMCs and communication technologies are marked in the figures to provide references for the devices that this type of self-powered technology may power.

the global photovoltaic market [18]. To achieve higher power conversion efficiency (PCE), the design of this type of photovoltaic technology has evolved from passivated emitter and rear contact cells to tunnel oxide passivated contacts, and now to silicon heterojunction solar cells [19]. Notably, Lin *et al.* introduced a nanocrystalline process to fabricate advanced hole-selective contact layers. When combined with a custom-designed transparent conductive oxide layer, this contact layer significantly enhanced the optoelectronic conversion efficiency of wafer-level single-junction silicon heterojunction SCs, achieving an impressive 26.81 % [20]. As the second generation of SC technology, thin-film photovoltaics represented by amorphous silicon materials have greatly reduced manufacturing costs due to their extremely thin film thickness foldability, and reduced use of silicon materials [21]. Furthermore, thin-film photovoltaic technology further reduces production costs by using flexible substrates and roll-to-roll production technology [22]. However, it should be noted that in thin-film photovoltaic technology, the bandgap values of the thin-film materials from bottom to top should gradually increase in order to fully utilize the entire spectrum of sunlight. For example, Li *et al.* introduced a Cd(O,S, Se,Te) layer near the front junction with the same crystal structure as the absorber, creating a bandgap gradient in Cd(Se,Te) SCs and achieving a PCE over 20 % [23]. Among the third-generation SCs, perovskite photovoltaic technology has attracted widespread attention due to its low cost, simple process and high PCE. Perovskite SCs are multilayer structures in which the perovskite layer is sandwiched between an electron transport layer and a hole transport layer. By improving perovskite crystallization methods, modifying perovskite interfaces, and optimizing charge extraction materials, laboratory-fabricated devices can achieve PCEs above 25 %. Among these, the hole transport material extracts photogenerated holes by blocking electron injection and suppressing charge recombination, which significantly enhances the optoelectronic performance and long-term stability of perovskite photovoltaics. Zhou *et al.* reported an organic hole transport material-T2, based on sulfur-methyl-substituted fluorenyl arms and a spiro core, which demonstrated enhanced hole extraction and reduced interface recombination. Perovskite SCs based on this material achieved a PCE of 26.41 % [24,25]. More importantly, the research on indoor photovoltaic cells has never stopped, providing more options for powering wearable biosensors [26]. When tested under low light levels (200–1000 lx indoor illumination conditions), multiple indoor photovoltaic cells based on perovskite and GaAs materials have already achieved the PCE exceeding 20 % [27–29]. Using liquid-phase processed SnO_2/MgO as a composite electron transport layer, the interfacial carrier recombination of an indoor perovskite SC was effectively reduced, while its stability was improved. Under 400 lx indoor lighting, the perovskite SC achieved a PCE of up to 26.9 % [27].

Although perovskite-based solar cells have made remarkable progress in photovoltaic conversion efficiency, these materials still have several limitations. Firstly, they exhibit sensitivity to humidity, thermal instability, and light-induced degradation [30]. For instance, methylammonium lead iodide is highly hygroscopic and decomposes into ineffective compounds upon exposure to moisture. Lead-based perovskite materials undergo light-induced degradation under high temperature and prolonged light exposure, leading to the loss of organic ammonium groups and consequently affecting their optoelectronic performance [31]. Secondly, most high-performance perovskite materials contain lead. Furthermore, the fabrication of perovskites often involves toxic solvents such as N,N-Dimethylformamide and Dimethyl Sulfoxide, which pose potential risks to the environment, as well as to animals and plants [32]. Additionally, during the large-scale fabrication of perovskite thin films, it is challenging to ensure the consistency of film quality, which still presents difficulties for large-scale production [30].

In self-powered wearable biosensor systems, third-generation photovoltaic technologies such as perovskite SCs, organic and dye-sensitized SCs are the main force in energy supply [33–47]. In a laboratory test environment, the main factor affecting the performance of the wearable SC is the input light intensity, which ranges from a few hundred microwatts to a few hundred milliwatts per square meter (Table 1). Therefore, the strategies to improve the performance of wearable SCs are mainly achieved by optimizing materials, structures and photoelectric conversion processes, which generally include bandgap matching, interface engineering and defect passivation, multilayer structures, enhanced light absorption, development of new materials or the application of multiplication engineering, etc [26]. These methods can not only improve the photoelectric conversion efficiency of wearable SCs, but also ensure their stability under low light conditions or during long-term wear. For example, by matching the cell bandgap with the indoor light spectrum, employing multiphase engineering to achieve phase stability and suppress halide segregation, and utilizing a minimal number of tandem cells, wearable perovskite photovoltaic cell designed for indoor use can generate 14.5 μW of power for wireless temperature sensing [48], even under ambient light with an input intensity as low as 0.16 mW cm^{-2}. In indoor applications, where the light intensity is relatively low and the spectrum is dominated by visible light, precisely tuning the material's bandgap to suit indoor lighting conditions enhances light absorption and efficiency. Additionally, suppressing the halide phase segregation maintains uniformity and structural stability in the perovskite material. A tandem structure, on the other hand, improves efficiency by enabling broader spectral absorption. Furthermore, Min *et al.* matched the bandgap of the SC with the indoor light spectrum and employed a large organic spacer (α-methylbenzylamine) to facilitate the formation of quasi-two-dimensional perovskite structures with large grain sizes and improved defect passivation [37]. This approach successfully led to the design of a high-performance wearable SC (0.165 cm^2), achieving a remarkable PCE of 31.2 % under illumination from a light-emitting diode (LED) with an intensity of 600 lx (0.215 mW cm^{-2}) [37]. In the effective area of 0.04–30 cm^2, the PCEs of wearable SCs are 5 %-30 %, and the output power is mostly concentrated between 0.1 and 10 mW (Fig. 2**A** and Table S1) [33,40–50]. Moreover, a jacket (244.55 cm^2) based on wearable SCs generates more than 1200 mW of electrical power [38].

As shown in the power output diagram of Fig. 2**A**, compared to the output power generated by all self-powered technologies (black dashed envelope), the output power (1.5–3.3 mW) of wearable SCs in the effective area range of 0.04–2 cm^2 is very impressive [46,47]. Therefore, thanks to the strong output performance and unified evaluation criteria, wearable SCs have developed rapidly and can be easily integrated with most commercial sensors (smart watches [33], sweat detectors [37], electronic implants [45], UV detectors [51], etc.), making an important contribution to the development of all-in-one self-powered wearable biosensor systems. However, SCs also face many obstacles on the road to powering biosensors, including the requirement for stable high-power output under low light conditions, toxicity issues and cost issues during manufacturing. Additionally, perovskite SCs face significant challenges in terms of film uniformity and device stability due to issues like solution processing technology, the interaction between substrates and interfaces, high sensitivity of perovskite materials to moisture, and thermal instability [52,53]. These challenges have a considerable impact on their industrialization.

2.2. Biomechanical generators

Harvesting biomechanical energy from human motion and visceral activity is a promising approach to power wearable biosensors. Taking an 80 kg person walking as an example (frequency, 1 Hz), the power generated by the heel strike is about 2 W [54]. With the automatic brake installed, the knee and ankle can generate a maximum power of 34 W and 20 W respectively [54]. Moreover, each second of exhalation and pulse beat generates nearly 1 W of power [55]. Despite the difficulties in harvesting these distributed biomechanical energies, TENG and PENG have excelled in converting them into electrical energy.

Through the coupling of the triboelectric effect and electrostatic

Table 1
Performance of self-powered technologies for all-in-one wearable biosensors[129–159].

Technologies	Solar cell	TENG	PENG	EMG/EF	E-BFC	TEG	MEG	HG	
Main factors	Light intensity: 0.16–348 mW cm^{-2}	Frequency: 0.1–4 Hz, ~kHz (ultrasound)	Frequency: 0.1–5.3 Hz	Frequency: EMG: 0.5–4 Hz EF: 1 kHz–10 GHz	Concentration: 0.2–300 mM	ΔT: 2.3–80 K	RH: 20 %–90 %	-	
Area (cm^2)/ Volume (cm^3)	0.04–244.55 cm^2	0.363–100 cm^2 1.53–48 cm^3	2.25–4 cm^2	EMG: 19.63–76.98 cm^2 16.617–122.15 cm^3 EF: 2.4–100 cm^2 0.002625–38.49 cm^3	0.006–30 cm^2	0.158–128 cm^2	0.01–3255 cm^2	1–76.06 cm^2	
Power/ Power density	DC ~1282.57 mW ~19.38 mW cm^{-2}	AC (peak) ~1076 mW ~420.3 mW cm^{-2}	AC (Peak) ~42.55 mW ~19.1 mW cm^{-2}	AC EMG: ~23.35 mW ~0.826 mW cm^{-2} EF: ~3480 mW ~207 mW cm^{-2}	DC ~10.5 mW ~3.7 mW cm^{-2}	DC ~419.8 mW ~100 mW cm^{-2}	AC/DC ~37.758 mW ~103.13 mW cm^{-2}	AC/DC ~195 mW ~30.96 mW cm^{-2}	
Pros	✔ High power ✔ High integration ✔ Unified evaluation criteria	✔ Extensive material selection ✔ Various structural designs ✔ Flexible device size		✔ High power ✔ Flexible device size ✔ High integration	✔ High integration ✔ Small device size	✔ High power ✔ Commercialization ✔ Unified evaluation criteria	✔ High softness ✔ Stretchability ✔ Large-scale manufacturing	✔ Collecting various energies	
Cons	• Limited by ambient conditions • Unstable output	• Moderate integration • Low average power • High impedance		• Tissue heating • Signal crosstalk • Confined to the energy emitting environment	• Low power • Low life cycle • Request to maintain fuel supply	• Flexibility • Stretchability • Moderate integration	• Low power • Conditional recycling • Moderate integration	• Low integration	
Refs.	[13–53]	[8,56–79]	[80–92]	[9,93–128]			[54,160–182]	[183–201]	[94–100, 127, 202–209]

ΔT, temperature difference. AC, alternating current.

induction effect, the relative movement between the two materials with different electronegativity in TENG leads to the gain and loss of surface charge, thus forming a potential difference (Fig. 2**B**) [56,57]. The charges flow through the external circuit to balance the potential difference, generating electrical energy. In general, TENG has four basic working modes, including contact-separation mode, single-electrode mode, horizontal sliding mode, and independent layer mode, among which the self-powered integrated wearable biosensor systems are more inclined to the first two modes [58–62]. Moreover, the wide range of material choices (from organic polymer films to common solid inorganic materials) and low-frequency adaptability (usually 0.1–4 Hz) enable TENG to harvest energy not only from the vitro motion but also from internal organs [60,63–70]. Notably, Hinchet *et al.* utilized a single-electrode mode TENG to capture mechanical energy transmitted by ultrasound (20 kHz) through the skin and liquid [71]. The vibration of the ultrasound on the skin caused the perfluoroalkoxy film on the TENG to contact and separate from the electrode, resulting in the charge gain and loss, producing current output in the external circuit. This demonstrated a novel method for powering implantable devices. Although there is a wide variety of commonly used triboelectric materials, the dielectric materials used to construct high-performance devices still have some limitations. Firstly, the triboelectric effect is highly dependent on the friction series, meaning that specific material combinations are required to produce high-output devices [64]. Secondly, due to the working mechanism, repeated friction between dielectric materials can lead to surface wear, resulting in a limited material lifespan [57]. Additionally, some commonly used materials, such as PTFE and nylon films, are difficult to degrade, posing potential environmental pollution concerns. Based on the flexible structural design, the effective area of TENG-based wearable devices ranges from 0.3 to 100 cm^2 and the volume is below 50 cm^3 (Table 1) [8,59–61,67–77]. Generally, by optimizing materials, structures, and working principles, wearable TENGs can achieve improved performance and a comfortable wearing experience. The specific strategies are as follows: 1) Use elastic and adaptable materials, or modify material surfaces with micro-nano structures to increase its surface area, enabling the wearable TENG to work stably in various environments. For instance, Yeh *et al.* utilized highly elastic liquid metal and microstructured Ecoflex materials as friction materials for contact-separation TENGs, achieving high charge transfer and long-term stability [60]. The surface of the flexible, soft, and biocompatible Ecoflex polymer was modified to resemble the structure of biomimetic shark skin, endowing the wearable sensor with high conformability as well as unique hydrophobic and anti-adhesive properties. 2) Use arrayed, flexible or adjustable structures to enhance output power and contact effect. 3) Perform energy management to optimize usage efficiency. A flexible contact-separation direct current (DC) TENG with a built-in switch to control circuit conduction achieved an instantaneous power of over 1000 mW and a power density of up to 420 mW cm^{-2}, which is 23900 times that of a conventional TENG without a switch [8]. However, the alternating current (AC) pulse output characteristics and low PCEs make the power output of wearable TENG concentrated in 0.1–7 mW (Fig. 2**B** and Table S1) [69–71,74,76]. Compared with the power envelope (black dashed line) based on all self-powered technologies, the power output of TENG is closer to the lower right corner of Fig. 2**B** (power-area plot), which means that the power density of the most wearable TENG is relatively low (maintained at 0.1 mW cm^{-2}). Therefore, methods such as material modification, environmental control, and charge excitation are employed to enhance the charge density of TENG, thereby increasing power output [78,79].

Unlike TENG, the material options for wearable PENG are relatively limited, primarily focusing on piezoelectric materials such as lead zirconate titanate (PZT), arrayed zinc oxide (ZnO) nanowires, and polyvinylidene fluoride (PVDF) films [80–85]. Based on the piezoelectric effect, when the piezoelectric materials are deformed by the external force, the centers of positive and negative charges in the unit cell no longer coincide, resulting in macroscopic polarization of the crystal and opposite charges appearing at both ends of the piezoelectric material (Fig. 2**C**) [85]. In 2006, Wang *et al.* demonstrated the first PENG [86]. The nanogenerator is composed of ZnO nanowires and Pt electrodes. Based on the piezoelectric effect, ZnO nanowires undergo internal polarization when deformed by external pressure. The Pt electrode induces opposite charges by contacting the ZnO nanowire surface, forming a potential difference that generates charge flow in the external circuit. It is important to note that the commonly used piezoelectric materials still have some limitations. Firstly, the stability of typical piezoelectric materials is relatively poor. PZT materials are brittle and have high rigidity [80]. ZnO nanowires are prone to fracture or fatigue under repeated mechanical stress [86]. PVDF is susceptible to thermal decomposition or performance degradation at high temperatures, and long-term use may lead to material aging and a decrease in piezoelectric performance [82]. Secondly, these piezoelectric materials have strong processing dependencies. For example, the piezoelectric performance of PVDF is highly dependent on the control of crystallinity, and the fabrication process requires high precision [82]. Therefore, improving the performance of wearable PENGs primarily involves enhancing the piezoelectric effect, increasing energy conversion efficiency, and boosting charge collection and storage capabilities. For example, selecting efficient piezoelectric materials or optimizing materials through polarization treatment [82]. Further optimization can be achieved by enhancing deformation capability or employing a multilayer design. For example, Xu *et al.* arranged porous piezoelectric ceramics with microstructures into ordered macroscopic array structures [80], successfully integrating multiple sensing units within a small area (2.23 cm^2) to construct a high-performance flexible PENG. The porous, layered piezoelectric ceramic elements optimized sensing and collection performance, while the array structure generated high levels of effective strain, and the use of piezoelectric composites enhanced device flexibility, achieving a power density approaching 20 mW cm^{-2}. With device areas less than 5 cm^2, most wearable PENGs operate at frequencies between 0.1 and 5 Hz, and output powers less than 50 mW (Fig. 2**C**, Table 1 and Table S1) [80,82–85,87–89].

Compared with other self-powered technologies, biomechanical energy generators based on TENG and PENG can choose environmentally friendly and non-toxic materials to form power-generating units or be implanted in organisms [90,91]. However, the pulsed output characteristics and large internal resistance (10–100 megohms) result in low PCEs and average power density, which leads to the fact that these biomechanical energy generators are often combined with other generators to generate electricity [92].

2.3. *Electromagnetic generator and wireless power transmission technology based on electromagnetic field*

In addition to TENG and PENG, the EMG is also suitable for harvesting biomechanical energy. Based on electromagnetic induction, when the magnetic flux in a closed circuit changes, an induced current is generated in the closed circuit (Fig. 2**D**). Wearable EMG mainly drives the movement of the magnet through the movement of the body, and then the coil damping converts the mechanical movement energy of the magnet into electrical energy [93]. As a mature energy harvesting device, wearable EMG outputs high power (up to 140 mW), accompanied by the characteristics of large current (up to 70 mA), small voltage (about 10 V) and small load (below 4000 ohms) [93–100]. Even though EMG prefers to collect high-frequency (greater than 5 Hz) energy, the operating frequency of wearable EMG bound to the joints makes it difficult to meet this requirement [101,102]. Not to mention the difficulty of reducing the effective area and volume of EMGs (20–80 cm^2, 20–130 cm^3). The power density of EMG is below 1 mW cm^{-2}, as shown in Table 1 [93–100]. Therefore, wearable EMG is often combined with other energy harvesters to form a HG for energy collection or motion sensing, which will be described in detail below in the following sections.

However, the energy obtained from the natural environment and the human body is still limited, which makes it difficult to cope with some wearable sensors with high energy requirements (such as blood oximeters). The wireless power transmission technology based on electromagnetic field (WPT-EF) is an excellent alternative, with the characteristics of convenient charging, contactless, more hygienic and longer autonomy. The principle can be briefly described as follows: electromagnetic waves generated by the time-varying electromagnetic field are collected across space by a receiving device (such as an antenna) [103]. The receiving device then supplies the collected energy to the load (Fig. 2**D**). Moreover, wireless power transmission (WPT) and wireless signal transmission operate on the same principle, except that the former focuses on transmitting energy, while the latter focuses more on the information in the energy transfer process. WPT-EF technologies can be divided into near-field (frequency, kHz to MHz), mid-field (MHz to GHz) and far-field (MHz to GHz) energy transmission [104].

For near-field energy transmission, power can be transferred via inductively coupled magnetic fields or capacitively coupled electric fields, and the transmission distance is generally in the order of millimeters or centimeters [105–110]. In inductive coupling, transmitting coils with large areas can effectively solve the problem of low energy transfer efficiency caused by angular misalignment and increased distance between the transmitting coil and the receiving coil. However, large transmitter coils (4–100 cm^2) do not prevent inductive coupling technology from transmitting high-power energy (10–3480 mW) [105–107,110]. Additionally, improving the stretchability and flexibility of the transmitting and receiving coils, while ensuring energy transfer efficiency, is a key foundation for developing flexible energy sources based on WPT-EF technology. Using flexible materials such as liquid metal, conductive polymers, and thin-film materials to fabricate transmission coils or flexible circuits is a common wearable design strategy. By filling channels temporarily formed and sealed by a sacrificial layer (such as polyvinyl alcohol film or tape) with liquid metals like Galinstan under negative or positive pressure, Teng *et al.* achieved high-resolution liquid metal patterning at different length scales [105]. The 7 cm diameter wearable wireless charging device achieved a power density of up to 90.43 mW cm^{-2} and a transmission efficiency of 60 %. Its power output is as high as 3480 mW, which is the maximum power output of all wearable self-powered technologies we have counted and is at the highest point of the power envelope. However, these flexible materials still have certain shortcomings. Firstly, liquid metals such as gallium and gallium-indium alloys are prone to the formation of an oxide layer on their surface, which can affect electrical conductivity [106]. Precise control over the shape and positioning of liquid metals requires complex microfabrication techniques, such as microchannel design. Additionally, some liquid metals (e.g., gallium) may have certain toxicity or evaporate at high temperatures, posing potential risks to the environment. Secondly, conductive polymers like polyaniline, and flexible films such as pure graphene films suffer from insufficient mechanical properties [111]. Under prolonged bending or stretching conditions, cracks or breaks in the conductive pathways may occur. Therefore, the chemical stability, conductivity and mechanical properties of flexible materials can be further improved by introducing anti-oxidation coatings and developing composite materials. Moreover, the use of embedded design or array structure design can disperse stress and extend the stress of devices and extend their life. Furthermore, the introduction of hermetic packaging or coating protection technology can also increase the service life of its devices. For mid-field energy transmission, based on magnetic resonance coupling, the transmitting and receiving devices have the same resonant frequency through reasonable calculations of coils and capacitances, which enables energy transmission over a longer distance and with higher efficiency [103]. Magnetic resonance coupling technology often powers electronic devices inside living organisms and can transfer milliwatt-level power to micro-implants in deep tissues (more than 5 cm) [112–116]. Based on this technology, Choi *et al.* developed a self-powered fully implantable cardiac pacemaker with a size of 2.4 cm^2 (volume, 0.06 cm^3), an energy transmission efficiency of 22.5 %, an output power of 100 mW, and a maximum transmission distance of 17 cm [116]. Furthermore, a novel mid-field energy transmission method transfers milliwatt-level power to micro-implants (2 mm, 70 mg) in deep tissues (>5 cm) for medical treatments such as physiological stimulation [112]. It uses patterned metal plates to induce adaptive energy transfer through propagation patterns in tissue and create a high energy density area deep in the tissue, which allows the energy harvesting structure to be made several orders of magnitude smaller than traditional pacemakers. However, the mid-field energy transmission based on magnetic resonance coupling faces difficulties such as complex technology, signal crosstalk, and large size. For far-field energy transmission, the energy is sent via radio frequency waves, captured by an antenna at the receiver end and converted into electrical energy to power the sensors. Radio frequency (RF) power transmission typically operates in the frequency range of 3 kHz to 300 GHz. In wearable systems, radio frequency technology is widely used for signal transmission [117–120]. Generally, RF power transmission efficiency can be effectively improved by optimizing antenna design, matching impedance networks, using advanced materials and intelligent algorithms, etc [103]. For example, by combining MoS_2 rectifiers with flexible Wi-Fi band antennas, Zhang *et al.* [121] have fabricated a fully flexible, integrated rectenna that enables wireless energy harvesting of electromagnetic radiation in the Wi-Fi band (~10 GHz) with a PCE of 40.1 %.

Moreover, based on electromagnetic induction, magnetoelectric materials enable millimeter-sized wireless stimulators. Similar to an induction coil, when the magnetic dipoles in the magnetoelectric material align with the external magnetic field, the magnetic field produces strain in the magnetostrictive layer, and this strain exerts a force on the piezoelectric layer, thereby generating a voltage [122]. Therefore, this magnetoelectric material-based WPT technology is different from those introduced previously, which converts the magnetic field into an electric field through mechanical coupling between the magnetostrictive layer and the piezoelectric layer. The ultra-small size (area, 0.06–0.27 cm^2; volume, 0.002–0.008 cm^2) of magnetoelectric materials combined with chip design can generate large output power (up to 56 mW and 207 mW cm^{-2}), making them deep implants (up to 5 cm) in the body for neural stimulation [9,122–125]. Kim *et al.* found that WPT based on magnetoelectric materials can increase power density by enhancing the adhesion between magnetoelectric material layers, clamping, and optimizing material thickness [9]. Based on these strategies, they can deliver 31 and 56 mW of power to magnetoelectric material receivers of 10 and 27 mm^2, achieving an energy density of 207 mW cm^{-2}. However, WPT technology based on electromagnetic materials has low conversion efficiency due to two energy conversions, and the external energy supplier (such as a battery) that provides the magnetic field makes it difficult for the overall device to be self-powered.

As shown in the power-area data in Fig. 2**D** and Table S1, in the size range of 0.001–10 cm^2, most of the energy output values of the wearable EMG and WPT-EF are on the power envelope formed by all self-powered technologies, indicating the ultra-high energy output (up to 3480 mW and 207 mW cm^{-2}). Power output in this range meets the needs of most low-power sensors, such as pacemakers, wireless cameras, etc [6,70,126,127]. However, for most wearable WPT-EF technologies, the main challenges faced include: 1) Coupling design of energy-receiving coil and living body. It mainly depends on the flexible materials used for coils, including polymers, graphene-based materials, and MXenes-based composites [111]. 2) Heating of biological tissues. Because organisms also absorb the energy transmitted by high-frequency strong electromagnetic waves (greater than 500 kHz, greater than 10 mT), leading to unsafe heating of biological tissues [128]. Therefore, it is especially important to study the energy transfer of low-frequency weak electromagnetic waves. 3) Signal crosstalk. Signal crosstalk may occur between electromagnetic waves of various frequencies, affecting the communication and energy transmission of WPT equipment. 4) WPT-EF

technology receivers always require additional energy-transmitting equipment, which brings difficulties to users in wild environments.

2.4. Enzyme-based biofuel cells

First proposed in 1964, the biofuel cell (BFC) consists of a dual-electrode cell separated by an electrolyte and is a subclass of fuel cells that use redox enzymes as catalysts [129]. Enzyme-based BFCs (E-BFCs) are attractive in the wearable field due to their abundant energy source. According to reports, the glucose concentration in relevant body fluids ranges for a healthy adult are as follows: 0.01–0.2 mM in sweat, 0.1–0.6 mM in tears, 0.24–0.72 mM in saliva, and 0.1–0.8 mM in urine [130–132]. Moreover, as the main metabolite of most tissues in the body, lactate exists at high concentrations (5–25 mM) in the sweat of healthy male bodies [133]. Based on these biological fluids, E-BFC can achieve in-situ power supply. The working mechanism of E-BFC is as follows: biofuels (e.g., glucose, lactic acid, etc.) are oxidized by oxidoreductase at the anode, and electrons flow through an external circuit to the cathode (direct current), where the oxidant (usually oxygen or peroxide) is reduced to water (Fig. 2**E**). Generally used oxidoreductases include cellobiose dehydrogenase [134], lactate oxidase [135], and bilirubin oxidase [136], etc [137]. The bioanode and cathode materials used include Au and Au nanotubes [134], graphite [135], platinum and their modifications [138]. Considering that E-BFCs primarily function in biological fluids, the functional materials used in E-BFCs should possess several essential characteristics, including biocompatibility, permeability, antifouling properties, conductivity, transparency, adhesiveness, and scalability. Biocompatibility refers to the ability of a material or device to interact with a biological system without causing significant adverse reactions [139]. This includes the immune and tissue responses during contact with the material, as well as the material's toxicity, stability, and degradability. Currently, natural materials such as cellulose and fabrics, as well as hydrogels like alginate and gelatin, exhibit excellent biocompatibility [139]. Surprisingly, the above two types of materials also have good permeability, which means that air and moisture can be exchanged through them, giving organisms a comfortable wearing experience. Additionally, by creating anti-contamination layers (such as materials like bovine serum albumin and polyethylene glycol) on the working electrode, high-performance anti-fouling materials can be formed, which prevent the binding of contaminants with the sensitive materials in the sensor during the reaction process, thereby preventing non-specific interactions [140]. However, such layers may hinder electron transfer, thus affecting the operational efficiency of the E-BFC. In addition, inorganic materials such as liquid metals, gold and graphene exhibit excellent electrical conductivity, and polymers like polydimethylsiloxane (PDMS) and polyimide demonstrate good transparency and adhesive properties [137]. However, these materials also have their respective limitations. Firstly, these functional materials cannot integrate biocompatibility, breathability, anti-pollution, conductivity and wearability. Materials such as gold and platinum are precious metals, making large-scale production economically unfeasible. The fabrication of nanostructures is complex, making it difficult to achieve mass production and consistent control [141]. Secondly, the electrical conductivity of materials like graphite is lower than that of metals, which limits their application as high-performance electrodes. Moreover, graphite has fewer active sites on its surface, which hinders the efficient immobilization of enzymes [137]. Therefore, to enhance the output power of wearable E-BFCs, strategies should be implemented to ensure the entire chemical reaction process is efficient and rapid. These strategies include increasing enzyme activity [142], modifying the electrode surface to promote electron transfer [143], and using high-surface-area nanomaterials to boost current density [144]. Additionally, by incorporating materials that enhance mechanical strength, such as carbon nanotubes, graphene, and self-healing polymers or hydrogels, the durability of E-BFCs can be improved after mechanical wear. The use of high thermal stability materials like polyimide and polydimethylsiloxane, along with coatings and encapsulation technologies such as polytetrafluoroethylene and epoxy resins, can mitigate the adverse effects of significant temperature and humidity fluctuations on the devices [139].

Therefore, Kwon *et al.* assembled gold nanoparticles onto cotton fibers layer by layer to form high-conductivity metal cotton fibers that serve as conductive carriers for enzyme-free cathodes and enzyme anodes [145]. Glucose oxidase was similarly assembled layer by layer onto the metal cotton fibers to become the anode. This method greatly enhanced the electrical communication between the enzyme and the electrode, and prepared a BFC with better performance compared to traditional devices. When the glucose concentration in sweat is 300 mM, the BFC with layer-by-layer assembled glucose oxidase-coated metal cotton fibers achieved a power density of 3.7 mW cm^{-2}, representing the best performance output among E-BFCs to date [145]. When the glucose concentration in sweat is 0.2 mM, the E-BFC based on liquid metal-based metal polymer conductors [146] produces a power density of 0.014 mW cm^{-2}. Thanks to technologies such as microfluidics and screen printing, E-FEC can be printed on PDMS, textile cloth and other soft base materials in the form of small-sized multi-units (0.006–30 cm^2), with a high degree of integration (Table S1) [145–159]. Furthermore, by utilizing the cross-dimensional integration of nanomaterials, Yu *et al.* reported an E-BFC that achieved a power density of 3.5 mW cm^{-2} in untreated human sweat at a lactate concentration of 40 mM [156]. Despite the high flexibility of E-BFCs, which allows for seamless integration with flexible electronic devices, low power output, limited life cycle, and the continuous need for fuel remain pressing issues for these energy harvesters.

2.5. Thermoelectric generator

In addition to metabolites being capable of generating energy, human bodies' thermal emissions are also an underestimated source of free energy. At room temperature of 25 ℃, an adult sitting still releases approximately 60 W of heat to the atmosphere through sensible heat transfer, while normal walking at a speed of 1.3 m s^{-1} releases about 100 W [54]. TEGs can convert this wasted energy into electrical energy. Based on the Seebeck effect, when the two sides of N-type and P-type semiconductors are exposed to different temperature environments, the internal carriers diffuse from the hot side to the cold side, generating the direct current in the external circuit connecting the two semiconductors (Fig. 2**F**). Semiconductor materials such as Bi_2Te_3, GeTe, PbTe, and their related alloys are traditional thermoelectric materials [160]. Among them, Bi_2Te_3 and its related dopants are currently the best-performing materials for thermoelectric applications at room temperature [161]. However, these thermoelectric materials still face some challenges in terms of cost, environmental impact, and stability. Both bismuth (Bi) and tellurium (Te) are scarce resources, and their high prices make the large-scale application of these materials economically unfeasible. PbTe contains lead, which poses significant environmental and health risks. At high temperatures, PbTe and GeTe are prone to chemical degradation or oxidation, which affects their long-term stability and reliability [161]. Therefore, it is very reliable to develop lead-free, low-toxic, environmentally friendly and low-cost thermoelectric materials, such as silicon germanium (SiGe) alloy, tin selenium (SnSe), etc. By adjusting the thermoelectric properties of materials through doping (such as adding Sb and Se to Bi_2Te_3) and alloying, the long-term stability and efficiency can be improved. The power generation efficiency of TEG is determined by the thermoelectric figure of merit of the thermoelectric material ($zT = \frac{S^2\sigma T}{\kappa}$) [162]. Under the condition of a certain temperature difference, high electrical conductivity (σ), high Seebeck coefficient (S) and low thermal conductivity (κ) mean high power generation efficiency. However, these three parameters are interrelated, making their simultaneous optimization extremely challenging. Therefore, at room temperature, most current wearable TEGs have zT values around 1

[161]. More importantly, the development of TEGs in wearable biosensors focuses on enhancing output power under limited dimensions at room temperature conditions [163].

Compared to TEGs for large-scale energy harvesting that have been tested at temperature differences of up to 80 K [164], wearable TEGs operate in environments with temperature differences of only 1–10 K [165–170]. Typically, wearable TEGs are composed of numerous micron-sized thermoelectric legs, with a total size ranging from 0.1 to 130 cm^2, capable of providing up to 419.8 W of power (Table 1 and Table S1) [164–181]. Based on a porous sandwich substrate and a directly welded copper foam heat sink, a new type of wearable TEG effectively improves the thermal conditions, greatly reduces the thermal resistance of the cold/hot side, and obtains high flexibility and 419.8 mW of power output [181]. Moreover, it integrates energy management, energy transmission, and signal transmission modules, functioning as a wearable multi-sensor health monitoring system. Based on the industrial silicon complementary metal-oxide-semiconductor process, Hu *et al.* fabricated a nanostructured silicon thermopile TEG with a total area of 48 μm × 36 μm and a power density of 33.33 mW cm^{-2}, which brings great opportunities for all-in-one wearable biosensors based on TEGs [163,182]. As illustrated by the power output in Fig. 2**F**, wearable TEGs demonstrate particularly outstanding energy harvesting performance within the centimeter size range. Therefore, by enhancing flexibility, stretchability, and integration with sensor chips, the TEG will become a more prominent energy harvesting technology in the field of wearable biosensors.

2.6. Moisture-electric generator

Moisture (water vapor), which is widely distributed in the natural environment, contains immense energy. Theoretically, 1 g of water transitioning from a gaseous to a liquid state can release 2260 J of energy, which is nearly equivalent to the energy contained in a standard AAA battery [183]. Based on the hydroelectric effect, electricity can be generated through the direct interaction between carbon nanostructured materials and flowing, dripping, and evaporating water [183]. Consequently, MEG has recently gained significant prominence in the field of wearable biosensors. In Fig. 2**G**, materials with gradient-arranged oxygen-containing functional groups adsorb water molecules from the air, resulting in a gradient distribution of H^+ ions [184]. Driven by this concentration gradient, the H^+ ions diffuse, generating current in the external circuit. In 2015, Qu *et al.* established an oxygen functional group gradient in a graphene oxide film [184], harvesting energy from the diffusion of moisture in the air, thus creating a pioneering moisture-powered generator with a PCE of up to 62 %. Later, Liu *et al.* discovered that protein nanowires could adsorb moisture from the air and generate charge separation through the interaction between the moisture and the nanowires [185]. The film devices made from these nanowires can continuously generate power spontaneously in the environment due to the self-maintaining humidity gradient. In addition to the commonly used graphene oxide materials, other active materials for MEGs include common polymers and their gels, such as polyacrylic acid (PAA), biomaterials like proteins, and semiconductor materials such as MoS_2 films [186]. However, these materials have limitations in practical applications. The hygroscopic properties of GO are highly dependent on environmental humidity, which restricts its use in environments with significant humidity fluctuations [186,187]. Additionally, GO has low mechanical strength and is prone to cracking or failure. PAA is a soft insulating material that is easily deformed or fractured, and must be combined with other conductive materials to enable charge transport [186]. Furthermore, the conductivity of MoS_2 is relatively low, limiting its charge transfer rate, and its production cost is high [186].

So far, research on wearable MEGs is still in the early stages of development [186]. The tested humidity environments typically range from 20 % to 90 % and most MEGs generate electrical power around 1 mW (effective area, 0.01–4 cm^2), as shown in Fig. 2**G** and Table S1 [184,188–197]. Therefore, efficient water capture ability and a long-lasting water gradient are crucial for achieving sustained high-power output in MEGs [193]. The former enhances ion diffusion, leading to higher power output, while the latter ensures continuous power generation. Current effective engineering methods include: physicochemical modifications to enhance surface hydrophilicity [195]; creating layered porosity to increase the contact area between materials and water molecules [184], thereby improving moisture absorption; forming internal chemical gradients through methods like laser irradiation to establish persistent water gradients [198]; and using asymmetric humidity environments to provide asymmetric moisture retention [199]. For example, Zhu *et al.* adjusted the surface charge and hydrophilicity of homemade protein films by changing the pH value of whey protein dispersion and applying plasma treatment [200]. A scalable MEG based on the film can generate around 30 mW of power at 40 % relative humidity (area range: 0.1–3255 cm^2). Due to the huge specific surface area and one-dimensional transport nanochannels, MEG based on gradient-doped polypyrrole nanowires has produced a high output power density of 103.13 mW cm^{-2}, demonstrating that accelerating ion transport can further optimize the performance of MEGs [201]. Based on the current research, if efficient MEGs can be manufactured with high power, high stability and adaptability to low-humidity environments, they would be compelling candidates for self-powered technology in the field of wearable biosensors.

2.7. Hybrid generator

Although some energy harvesters can meet the energy requirements of most low-power electronic devices, their output performance is mostly limited by the environment. SCs are limited in their application during the night. Harvesting biomechanical energy requires continuous triggering of devices. WPT-EF depends on an energy emitter, and BFCs require a continuous supply of biological fluids. In practical applications, HGs capable of simultaneously harvesting multiple types of energy can improve the cost-effectiveness of all-in-one systems significantly.

Based on the flexible structural design, TENGs are easier to integrate with other energy harvesters to form HGs. Theoretically, combining TENG with EMG can achieve higher power output, as the former has high voltage output characteristics while the latter provides high current output [94,96–99]. For example, a new HG with a volume of 16.617 cm^3 achieved an ultra-high power output of 112 mW by rationally integrating EMG with two working modes of TENGs [100]. During the capacitor charging process in HGs, EMG plays a primary role in the initial stages, while TENG becomes more significant in the later stages [94,96–100]. Additionally, the synergistic collection of biomechanical energy and solar, biochemical energy, etc. is also an attractive approach in HGs [95,202–205]. By assembling a hybrid power source made of an independent layered TENG from Ag and PET film and a polycrystalline GaAs thin-film SC, Yan *et al.* achieved a power density of up to 30.96 mW cm^{-2} (PCE, 30.75 %) [205]. Utilizing both mechanical motion and solar energy, the wireless physiological monitoring system based on this hybrid power source can further monitor the wearer's heart rate, blood pressure, temperature, and motion parameters. Based on the analysis of the capacitor charging process in most HGs, other generators contribute the most energy during turbulent charging, whereas TENG mainly provides energy for trickle charging [206]. Moreover, the integration of other energy harvesters opens up possibilities for diverse forms of energy collection [127,207–209]. For instance, a hybrid generator combining photothermal and thermoelectric conversion can output up to 195 mW of power under the cover of biological tissue [127]. However, harvesting energy from multiple sources also implies accumulating multiple energy harvesters, and unreasonable structural designs can lead to increased device size. By observing the output statistics (Fig. 2**H** and Table S1), it is evident that there is a high correlation between the power output of HGs and their

effective area. Therefore, further improving the structural design of HGs and enhancing the synergy between different energy harvesters are essential for developing the application potential of HGs in the field of wearable biosensors.

Overall, as shown in Fig. 1**B,** Table 1 and Table S1, the sizes of most wearable energy harvesters range from 0.01 to 100 cm^2, with power outputs spanning from 0.001 to 1000 mW. The highest and lowest power output points come from WPT-EF technology and E-BFC technology, respectively, which are determined by their working mechanisms, device structures, and energy sources. In Fig. 1**B** and Fig. 2, the technologies in the upper left corner of these power-size diagrams exhibit the highest power density. We anticipate that newly invented energy harvesting technologies or improvements to existing ones (we have already mentioned in the review of each self-powered technology) can achieve even higher power densities, expanding the power envelope in these figures further towards the upper left.

2.8. Energy management for self-powered technologies

According to Fig. 1**B**, although most of the surveyed energy harvesters can meet the power requirements of some low-power electronic devices, their actual performance in practical applications is often disappointing. It is primarily due to the mismatch between sensors and energy harvesting devices, making appropriate energy management essential. Generally, EMCs for self-powered technologies consist of three parts: rectifiers, the DC-DC conversion module including the maximum power point tracker (MPPT) and charging controller, and energy storage devices. Moreover, the inherent high-voltage, low-current output characteristics of TENGs necessitate the use of distinct EMCs compared to other energy harvesters (Fig. 3**A**).

2.8.1. Rectifiers

Before further utilizing the energy harvested by the energy collector, a rectifier must first convert the AC output into DC output, including the half-wave rectifier, the full-wave rectifier, the bridge rectifiers, and the voltage doubler circuit (Fig. 3**B**). A half-wave rectifier typically includes only one diode in the circuit, achieving rectification at the expense of losing half of the AC output. The half-wave rectifier has a simple structure and is often used to prevent current from flowing back from the energy storage unit to the SC [7], or as a charge replenishment channel in TENG applications [210].

Full-wave rectification utilizes the entire waveform of the AC signal, converting both half-cycles into DC, significantly improving rectification efficiency. It mainly consists of two types: the conventional full-wave rectifier circuit (using two diodes) and the bridge rectifier circuit (using four diodes). Using a conventional full-wave rectifier circuit, the maximum energy provided by TENG to a capacitive load is higher [211,212]. However, in a bridge rectifier circuit, each diode experiences a lower reverse voltage, making it the preferred choice for most energy harvesters [105,213].

Additionally, diodes with guiding properties, combined with capacitors with charging and discharging characteristics, form the voltage doubler rectifier circuit [214]. The working principle of the second-order voltage doubler rectifier circuit is as follows: during the positive half-cycle of the AC supply, the first diode conducts, charging the first capacitor. In the negative half-cycle, the second diode conducts, working in conjunction with the first capacitor to charge the second capacitor. As the capacitors accumulate charge, the output voltage ultimately exceeds the input voltage. This circuit can convert low-voltage AC signals into high-voltage DC output and has been widely applied in the field of TENGs [78,215]. Based on this mechanism, the contact-separated TENG works as a capacitor in the voltage doubler rectifier circuit, resulting in an exponential charge output. Further optimization of various parameters, including dielectric materials (thickness, type, etc.), environmental conditions (air pressure, oxygen, humidity, etc.), and adjustment of the voltage doubler rectifier circuit

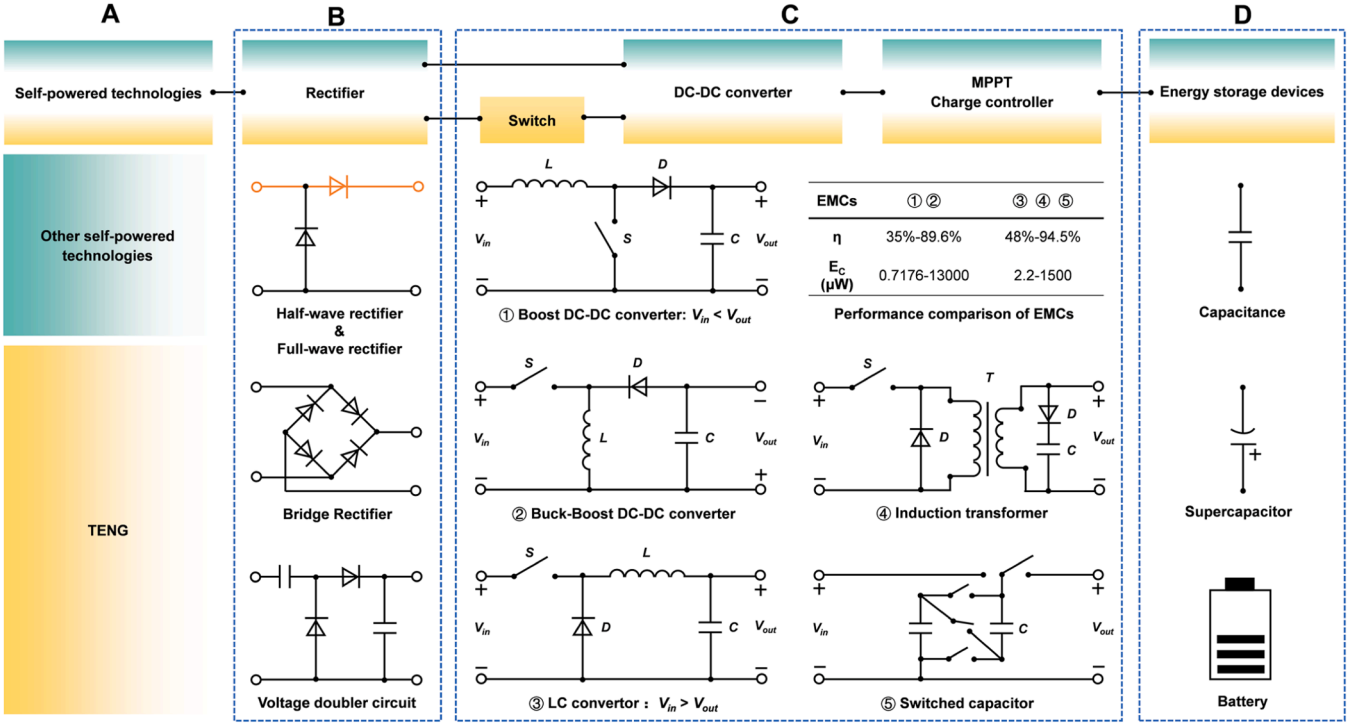

Fig. 3. Energy management circuits in self-powered technologies. (A) Different self-powered technology. Compared with other self-powered technologies, TENGs use different EMCs. (B) Different rectifiers. (C) Different DC-DC converters. The maximum power point tracking (MPPT) module and charge controller are placed in the more advanced DC-DC converters. DC-DC converters based on the hysteresis switch are more suitable for TENGs. The table summarizes the energy conversion efficiency and energy consumption of EMCs (including 5 types). (D) Different energy storage devices. DC, direct current. V_{in}, input voltage. V_{out}, output voltage. *L*, inductor. *D*, diode. *C*, capacitor. *S*, synchronous switch.

(order, capacitance, etc.) can significantly enhance the output charge density of excitation TENG [78], reaching up to 4.13 mC m^{-2}. The lower output efficiency and susceptibility to external disturbances indicate that there is significant room for improvement in voltage doubler rectifier circuits within the self-powered domain.

2.8.2. DC-DC converters

After the rectifier, the energy source from the energy harvester enters the DC-DC converter. Here, the DC-DC converter adjusts the input voltage to meet the requirements of subsequent energy management. The main electronic components of a DC-DC converter include inductors (*L*), diodes (*D*), capacitors (*C*), and synchronous switches (*S*), etc. Typical DC-DC converters are divided into boost type, buck type, and buck-boost type. Self-powered technologies such as SC, TEG, and E-BFC have a relatively small output voltage and often use a boost DC-DC converter, whose simplified schematic diagram is shown in Fig. 3**C** (①) [181,216,217]. First, the switch is turned on and the current in the inductor increases. Then, when the switch is turned off, the polarity of the inductor is reversed, and the inductor voltage is superimposed with the input voltage to form a total voltage higher than the input voltage. The superimposed voltage drives the current through the diode and the load to charge the output capacitor. However, because the environments in which these energy harvesters operate are not stable, such as changes in sunlight intensity and temperature affecting the output voltage of the energy harvesters, buck-boost DC-DC converters (②) are essential for self-powered technologies like SC [218], PENG [219], and TEG [220]. The mechanism is as follows: the switch is turned on and the current in the inductor increases. The output is now mainly maintained by the discharge of the capacitor. Then, the switch is turned off, and the current in the inductor flows to the load and capacitor, and then returns to the inductor after passing through the diode. In this circuit, the output voltage can be controlled by controlling the duty cycle of the switch. Currently, advanced manufacturing techniques have integrated the DC-DC converters, MPPT, and charging controllers into a single circuit board, resulting in commercialized products (BQ25504, LTC3108, etc.) [126]. Additionally, in the field of wearable biosensors, energy management strategies based on boost mode and buck-boost mode have energy conversion efficiencies ranging from 35 % to 89.6 % [126,127,165,167,168,173,176,181,221]. Depending on the energy consumption of the driven sensors, the energy consumption of this management strategy varies from 0.00072 mW to 13 mW [126,127,165,167,168,173,176,181,221], as shown in Table S2. It is worth mentioning that by using nanopower design technology to minimize the inherent consumption during operation, the fully autonomous power converter chip proposed by Dini *et al.* can be applied to a variety of energy harvesters, with a peak power conversion efficiency of up to 89.6 % and an inherent current consumption as low as nanoampere level [221].

Furthermore, buck DC-DC converters, which can reduce the voltage of the energy source, are highly compatible with TENGs. They are mainly classified into three types: LC converters (③) [222], inductor transformers (④) [223], and switched capacitors (charge pumps, ⑤) [224]. The most widely used are LC converters due to their simple structure and ease of manufacturing. However, TENGs are often incompatible with commercially available inductive components, necessitating the design of custom inductors for optimal performance. Based on this, Wang *et al.* proposed a general design procedure for matching inductors in electrostatic energy conversion, achieving a module energy conversion efficiency of 90.7 % and a total energy conversion efficiency of 81.6 % [222]. Similarly, issues with inductive transformers are resolved by using adjustable automatic spark switches and custom-made transformers, achieving an energy conversion efficiency of 78.5 % [223]. In recent years, switched capacitors, formed by series and parallel combinations of capacitor banks, have effectively demonstrated voltage conversion capabilities. They possess advantages such as being non-magnetic, highly efficient (greater than 94 %), and effectively enhancing charge, making them promising for applications in TENG, E-BFC and other related fields [224,225]. Specifically, Liu *et al.* developed a switched-capacitor converter based on a fractal structure. By reducing the negative impact of the total output voltage drop across the switches, it efficiently converts high voltage and low charge to low voltage and high charge, achieving an energy transfer efficiency exceeding 94 % in constant output mode [224]. The conversion efficiency of buck DC-DC converters ranges from 48 % to 94.5 %, with energy consumption between 0.002 and 1.5 mW (Table S2) [213,222–224,226–231].

Due to high internal impedance and pulse signal output, TENGs must employ switches to achieve low-frequency energy storage and instant energy release before employing the aforementioned buck DC-DC converters, avoiding significant energy loss [223,231]. Common switches include contact switches [229], electrostatic vibration switches [232], electric switches [233], triodes [228], plasma switches and discharge switches [234,235]. Furthermore, MPPT continuously adjusts the operating point of the energy source to maintain the maximum power output, while the charging controller manages the charging process of energy storage devices, extending their lifespan and ensuring safety [7].

2.8.3. Energy storage units

Finally, commercial capacitors, supercapacitors, or batteries are used to store the energy after management. Among them, supercapacitors with fast charging and discharging characteristics can provide stable power output, which complements the irregular current generated by the energy harvester and makes up for the energy fluctuations caused by the unstable working environment, which has attracted widespread attention [236,237]. Moreover, we have plotted the statistical power range consumed by EMCs in the wearable biosensor field near the y-axis in Fig. 1**B**. Since EMCs consume a significant portion of the energy captured by the harvesters, improving their energy conversion efficiency can further optimize the all-in-one self-powered wearable biosensors.

It is worth emphasizing that in recent years, machine learning, as an emerging approach, has maximized the optimization of the energy conversion process through its intelligent characteristics, thereby reducing energy loss and improving overall efficiency. Currently, machine learning-based energy management mainly focuses on the following three aspects. First, machine learning models such as time-series analysis or deep learning are used to predict changes in external environments such as light intensity or motion frequency, which in turn adjust the operating modes of self-powered devices. For example, using a radial basis function neural network algorithm to predict time-series data, Yona *et al.* were able to predict the power output of a photovoltaic system 24 hours in advance based solely on meteorological data, preparing for solar energy collection, management, and storage in advance [238]. Second, reinforcement learning or deep learning algorithms optimize the control strategies of energy converters, improving MPPT and energy conversion efficiency under different load conditions. For example, an algorithm based on linear and nonlinear regression machine learning is used to operate photovoltaic systems at their maximum power point, determining the duty cycle of boost converters to enhance energy conversion efficiency [239]. Third, in the case of multiple self-powered technologies coexisting, machine learning can analyze the output characteristics of each module in real-time and adaptively allocate energy to different energy storage modules or directly supply loads. Additionally, machine learning can dynamically adjust the operational modes of devices (such as sensor sampling frequency or communication intervals), minimizing power consumption while ensuring performance. For instance, using ultra-low-power edge computing, a TEG-based self-powered wearable system can estimate multi-modal health parameters, including time-varying metabolic energy, in real-time, detecting limb movement and skin temperature [167]. Therefore, the development of energy management circuits based on machine learning or adaptive energy routing will further enhance the operational efficiency of self-powered wearable biosensors.

3. All-in-one wearable biosensors

Self-powered technologies not only provide energy support for the integration of wearable biosensors, but they can also serve as active sensors, offering diverse pathways for signal acquisition. In this process, the cooperation with integrated engineering such as signal arrays, microfluidics, screen printing, integrated circuits, etc. enables a large number of signals to be collected and processed simultaneously, greatly simplifying sensor networks. Next, we will review wearable biosensors from the perspectives of mechanisms, size, performance, and integration technologies, with a particular focus on power consumption, wearability, sensitivity, and their improvement strategies (Fig. 4, Table 2 and Table S3).

3.1. Wearable biosensors

Wearable biosensors utilize biomaterials as recognition elements to convert biochemical reactions into quantifiable physical and chemical signals. By incorporating flexible substrates, they enable real-time, in situ sensing of various biological signals. The first generation of wearable biosensors primarily focused on biophysical monitoring by tracking an individual's physical activities or vital signs. Based on physical principles (such as electrical, optical, mechanical, and magnetic), biophysical sensors convert changes in biological systems (such as pressure changes) into measurable physical signals (such as voltage) [240]. Numerous biophysical sensors have already been commercialized [172]. The second generation of wearable biosensors primarily relies on biofluids, using biorecognition elements (such as glucose oxidase) to chemically react with specific analytes in the biofluids (such as glucose) to produce detectable signals (such as current) [241]. These biochemical sensors, which come in forms such as patches [242], contact lenses [243], and textiles [7], are mostly still laboratory prototypes. Currently, the development of wearable biosensors has gradually shifted from uniform medical monitoring towards personalized health services [244]. However, the pursuit of integration has never ceased.

3.1.1. Commercial wearable biosensors

Commercial wearable biosensors integrate signal collection, processing and transmission into one device, which can be easily connected to the energy harvesters to become the integrated devices. As shown in Fig. 4**A** and Fig. 1**B**, typical power requirements for most commercial low-power biosensors range from 0.005 to 100000 μW. Wherein, most commercial sensors are based on biophysical signals, including cochlear implants (power, 513–100 μW) [127,245], microphones (420–3632 μW) [126,246], thermohygrometers (0.005–10 μW) [172,181,247–250], accelerometers (2.4–2520 μW) [168,172], pressure sensors (30–1000 μW) [98,251,252], pulse oximeters (24–17000 μW) [6,11,181,253], electrocardiogram displays (50–100 μW) [153,172], LEDs (750–1100 μW) [173,213], etc. For example, a high-performance TEG combined with EMCs based on LTC3108 and BQ25570 can drive a blood oxygen sensor by harvesting thermal energy [181]. The sensor consumes 472 μW at a low operating frequency (1/30 minute), while real-time

A

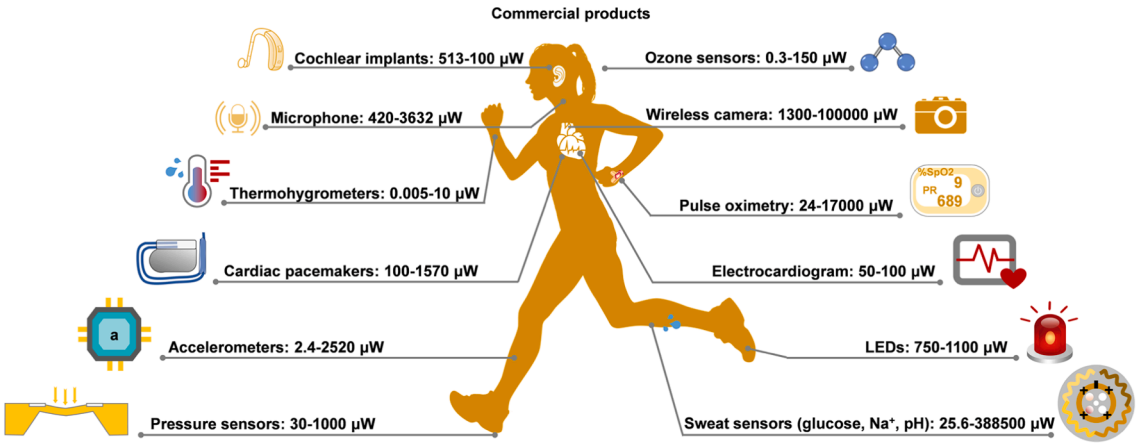

B

Active biosensors	Signal source	Size	Sensitivity	Applications	Technologies relied on
Biophysical sensors	Vital signs: ✓ Pulse ✓ Respiration ✓ Vocalization ✓ Temperature ✓ Pressure ✓ Heartbeat	0.01~10 cm^2 0.001~10 cm^3	0.0025-90.95 V kPa^{-1}	Personalized health care[70, 83, 89, 255, 256, 260-262]: ✓ Vital signal detection E-skins[75, 257, 263-270]: ✓ Tactile sensing ✓ Temperature sensing ✓ Pressure sensing Communication[12, 68]: ✓ Sign language interpretation ✓ Mechnosensational communication system Body motion monitoring[93, 258, 271-275]: ✓ Joint motion ✓ Hand motion ✓ Lower limb movement	TENG PENG EMG TEG MEG HG
			0.011-15.44 kPa^{-1}		
	Physical activity: ✓ Finger Touch ✓ Joint motion ✓ Eye motion ✓ Impacts		426.4-729 μV K^{-1}		
			Accuracy rate: 92.5%-99.8%		
Biochemical sensors	Biofluids: ✓ Sweat ✓ Tears ✓ Saliva ✓ Blood ✓ Urine ✓ Gastric fluid	0.01~50 cm^2 0.01~2 cm^3	0.0021~1 mV cm^{-2} mM^{-1}	✓ Glucose and lactate monitoring[117, 150, 277-281] ✓ Smart contact lens[118, 283] ✓ Gastric fluid leakage monitoring[282] ✓ Detection of multiple biomarkers[119, 259]	SC TENG WPT-EF E-BFC HG
			0.062-110 mV mM^{-1}		
			11.13-69.4 mV pH^{-1}		
			Accuracy rate: 96-99.543%		

Fig. 4. Commercial and active wearable biosensors. (A) Classification and power consumption range of common commercial products based on wearable biosensors. (B) Comparison of active biosensors based on self-powered technologies. LEDs, light emitting diodes.

Table 2
Comparison of all-in-one integrating technologies for self-powered wearable biosensors.

Technologies	Signaling array	Microfluidic technology	Screen printing	Integrated circuit
Mechanism	Integrating multiple signal units	Systems that process tiny fluids using microchannels with dimensions ranging from tens to hundreds of micrometers	A technology that uses some meshes to pass ink and other meshes to block ink, thereby printing the designed graphics	A set of electronic circuits on a small flat piece of the semiconductor material
Base materials	✔ Conductive carbon fibers ✔ Silicone, cotton, PET, PDMS, PVDF, TPU	✔ PDMS, PET	✔ Graphene, carbon nanotube, liquid metal, Au, metallic cotton fiber ✔ Paper, glass, PET, polyimide tape, PDMS, textile	✔ Polyimide, polyester film, epoxy resin, parylene
Targeted parts	• Energy harvesting • Signal acquisition • Signal processing • Signal transmission	• Energy harvesting • Signal acquisition • Signal processing	• Energy harvesting • Energy storage • Signal acquisition • Signal processing • Signal transmission	• Energy harvesting • Energy management • Energy storage • Signal acquisition • Signal processing • Signal transmission
Degree of integration	Identifying dozens of signals Integrating hundreds of units	Identifying several signals Integrating dozens of units	Identifying several signals Integrating hundreds of units	Identifying several signals Integrating several parts
Packaging	Both	Yes	No	Both
Pros	✔ Simultaneous collection of biophysical signals ✔ Simple technology ✔ Precise control signals ✔ Rapid response and on-site analysis ✔ Parallel processing and collection biochemical signals	✔ Low-cost, large-scale production ✔ Simple technology, various materials ✔ Soft, conformable, and reducing sensor thickness	✔ Miniaturization ✔ Low power consumption ✔ High performance ✔ Reliability and durability	
Cons	• Signal crosstalk • Multiple units mean large volumes	• Material Limitations • Complex and expensive manufacturing • Disposable	• Ink uniformity • Low pattern accuracy • Electronic components are hard to print	• Limited flexibility • Complex fabrication • Heat dissipation
Applications	Signal integration	Signal integration	Component integration	Signal and component integration
Ref.	[8,66–68,73,89,166,171,256,264,270,273,275,285–287]	[61,155,156,196,278,280,281,288–290]	[106,145,146,148,150,151,153–155,158,189,200,291–297]	[45,46,61,65,72,76,77,83,84,156,171,298–302]

PET, polyethylene terephthalate. PDMS, polydimethylsiloxane. PVDF, polyvinylidene fluoride. TPU, thermoplastic polyurethanes.

operation requires 17000 μW of power. It should be noted that the wearer's physical state (static or dynamic), the sensor's computing mode (edge computing module or real-time transmission module), and the signal transmission method (wired or wireless transmission) seriously affect the sensor's power consumption [167]. Sometimes, these factors can cause the power consumed by sensors to differ by two or more orders of magnitude, making the above sensor energy consumption values have a range. Moreover, ozone sensors (0.3–150 μW) and sweat sensors (25.6–388500 μW) are based on biochemical signals [37,118,172,241,254]. Among them, the emerging sweat sensors have not only attracted the interest of researchers in recent years, but also commercial products have been launched, including Epicore Biosystems' Gx Sweat Patch, Nix Biosensors, and Philips Health Watch [3]. Although these commercialized sweat sensors do not disclose specific power consumption parameters, recent research indicates that the more sensing signals and higher integration a sweat sensor has, the higher its energy consumption [241]. Additionally, implantable devices like cardiac pacemakers and endoscopes with wireless cameras can still be powered by energy harvesters with the assistance of EMCs, even though they have relatively high-power consumption (the former, 100–1570 μW; the latter, 1300–100000 μW) [6,35,70,126,127].

In summary, these low-power commercial biosensors have gradually realized signal sensing from in vivo to in vitro. The energy consumption ranges of commonly used biophysical and biochemical sensors are recorded on the two vertical lines near the y-axis in Fig. 1**B** for reference in subsequent self-powered biosensors. However, the limited power output of energy harvesters and the growing market demand for personalized and multifunctional sensing have prompted the development of more active sensors.

3.1.2. Active wearable biophysical sensors

Currently, wearable active biophysical sensors are mainly based on various energy harvester technologies, including TENG, PENG, EMG, TEG, MEG, and HG. Signal sources range from vital signs of organisms to body activities, including pulse, breathing, sound, body temperature, heartbeat, various joint movements and external impacts. Based on physical effects such as piezoelectricity and triboelectricity, the epidermal strain caused by these vital signs and human body movements generates electrical signals (such as voltage, current, etc.) through changes in the properties of the sensor material [3]. Taking the TENG-type active physical sensor as an example to explain the principle, when the force applied to the TENG increases, the effective contact area between the triboelectric layers enlarges, resulting in a higher voltage output signal. Therefore, the parameters used to characterize the sensitivity of biophysical sensors are often expressed in units such as V kPa^{-1}, kPa^{-1}, and μV K^{-1}. Furthermore, with the rise of artificial intelligence, machine learning can extract and analyze deeper and more subtle sensor information, thereby achieving intelligent identification, control and decision-making, making accuracy another indicator of sensitivity. For example, Kong *et al.* designed a self-powered, self-sensing lower-limb system that harnesses energy from walking using a half-wave EMG while accurately detecting the knee joint's rotation angle and direction through a three-channel TENG based on binary encoding [93]. The system utilizes a deep learning predictive model (long short-term memory) to extract feature signals from TENG output, achieving a recognition accuracy of 99.68 % and a motion detection accuracy of 99.96 %. It demonstrated capabilities in detecting movements such as falls, sitting, balancing, and walking, making it highly suitable for rehabilitation applications. The sensitivity ranges for all movements are illustrated in Fig. 4**B**. Although the sensitivity of the sensors is heavily affected by various factors such as the sensing principles, sensing materials, structural design, and signal processing, it can be significantly enhanced through optimization of material properties, increased contact areas, noise reduction, integration of multimodal

sensing technologies, and the adoption of advanced miniaturization and flexible designs. The pursuit of highly sensitive wearable biophysical sensors is also part of the all-in-one engineering. By introducing a third phase at the particle-polymer interface, Peng *et al.* increased the relative dielectric constant of the triboelectric layer and suppressed its dielectric loss [75], obtaining a TENG-based wearable sensor with a pressure sensitivity of 90.95 V kPa^{-1}. To achieve more precise sensing, the unit area and volume range of biophysical sensors are 0.01–10 cm^2 and 0.001–10 cm^3 respectively [83,255–259]. Among them, based on inorganic laser lifting technology, Park *et al.* transferred high-quality piezoelectric film to ultra-thin PZT to form a piezoelectric pulse sensor (thickness 4.8 μm) [260]. The ultra-thin piezoelectric pulse sensor achieves conformal contact with the skin texture and can respond to tiny pulses generated on the epidermal surface (sensitivity of 0.018 kPa^{-1}, response time of 60 ms), with a volume as small as 0.00048 cm^3.

Ultimately, active biophysical sensors enable personalized healthcare by detecting vital signs [69,70,83,255,256,260–262], create e-skins through tactile, temperature, and pressure sensing [75,257,263–270], facilitate communication through sign language translation and mechanical sensing [12,68], and monitor human movement by capturing various joint motions [89,258,271–275].

3.1.3. Active wearable biochemical sensors

Biological fluids, such as sweat, tears, saliva, blood, urine, gastric juice, etc., provide a rich signal source for active wearable biochemical sensors. SC, TENG, EF, E-BFC, and HG provide energy support for active biochemical sensors. Generally, active biochemical sensors can detect dynamic changes in biomarkers such as ions and metabolites through techniques like potentiometry, amperometry, voltammetry, and impedance spectroscopy [276]. These sensors can diagnose individual biological diseases by monitoring glucose [117,150,277–281], gastric juice [282], etc [119]. Compared to active biophysical sensors, biochemical sensors generally have a larger effective surface area (0.01–50 cm^2) but a smaller effective volume (0.01–2 cm^3) [117,118,279,280,283]. This is because most active biochemical sensors are powered by EF and E-BFC, and a larger surface area allows for more energy reception and provides a greater area for chemical reactions. Additionally, the sensitivity of active biochemical sensors is primarily characterized by the ratio of the obtained voltage value to the concentration of the involved biomarkers. The units commonly used to express this sensitivity are mV cm^{-2} mM^{-1}, mV mM^{-1}, and mV pH^{-1}. Enhancing the sensitivity of active wearable biochemical sensors requires a multifaceted approach involving material optimization (using highly conductive and catalytically active materials), surface functionalization (attaching specific antibodies and enzymes to the sensor surface), structural design (employing miniaturization and nanoscale materials to improve spatial resolution), increasing sensor surface area (by using nanomaterials), and signal enhancement (through electrochemical amplification or optical enhancement techniques) [51,117–119,150,277–284]. These improvements lay the foundation for detecting biochemical molecules at lower concentrations, enabling real-time and precise monitoring. Huang *et al.* reported a stretchable self-powered sweat sensor with an epidermal electronic format, in which the E-BFCs serve as both the energy sources and the sensing modules [279]. They enhanced the sensor's stretchability and uniformity by spraying graphene on gold electrodes and designing it into an epidermal shape for comfortable, skin-worn, continuous, real-time monitoring. This biosensor achieved in-situ detection of lactate with a sensitivity of 2.48 mV mM^{-1} and glucose with a sensitivity of 110 mV mM^{-1}. Furthermore, a power-free smart contact lens utilizes an electrochromic material (Prussian blue) as the electrode to enable non-invasive glucose sensing [283]. In the presence of oxygen, glucose oxidase acts as a catalyst to oxidize glucose in tears into gluconic acid and H_2O_2. The H_2O_2 induces the electrochromic material to transition from its reduced to oxidized state through the transfer of Na^+ and K^+, causing the Prussian blue to change from transparent to blue. The greater the glucose concentration, the more significant the color change of the Prussian blue. With the integration of image processing and machine learning algorithms, the contact lens achieves a high correlation coefficient of 0.99543 and can detect glucose concentrations as low as 0.05 mM.

3.2. All-in-one integrating technologies for wearable biosensors

Active biosensors and commercial wearable products enable precise medical care and personalized monitoring for individuals. However, whether it involves the collection, processing, and storage of energy or the collection, processing, and transmission of signals, engineering integration is essential. Therefore, the trade-offs between performance metrics and all-in-one integrating technologies deserve further discussion and summary. Here, we summarize four all-in-one integrating technologies for self-powered wearable biosensor systems, focusing on the mechanism, materials, target parts, degree of integration, advantages, and disadvantages: signal array, microfluidic technology, screen printing, and integrated circuit (Table 2).

3.2.1. Trade-offs between performance metrics during integration

The integration of self-powered wearable biosensors is not merely a matter of combining energy modules and sensing modules. It is more akin to the all-in-one design of a complete system, requiring careful trade-offs between the device's performance metrics. Here, we focus on discussing the trade-offs between three key pairs of performance metrics (Table S3), including power density versus flexibility, sensitivity versus durability, size versus integration. Furthermore, we summarize strategies for balancing these competing factors and explore the implications of these strategies for the future integrated design of self-powered wearable biosensors.

During the integration process, there is a trade-off between the output power of the device and its own flexibility. In general, flexible or stretchable materials, such as thin-film solar cells, flexible triboelectric materials, piezoelectric materials, stretchable conductive metals, or liquid metals, are commonly used to improve the comfort of wearable biosensors [51,75,89,119,150,265,266,268,269]. However, these flexible materials may exhibit lower power output performance in certain cases. For example, in the comparison of pressure sensors or electronic skin based on TENGs and PENGs, their sensitivity is typically expressed in V kPa^{-1}. Mahanty *et al.* effectively improved the output power of PENGs to 0.362 mW cm^{-2} by using a heterostructure of piezoelectric composite nanofibers and gap metal sheets [89]. However, the combination of multilayer piezoelectric films undoubtedly reduced the comfort, while the sensitivity of the PENG-based device was 20 ± 1.4 V kPa^{-1}. In contrast, Peng *et al.* enhanced the relative dielectric constant of the dielectric material and suppressed dielectric loss by using a nanometer-scale design of the polymer interface [75], resulting in a self-powered pressure sensor with a sensitivity of 90.95 V kPa^{-1} and a power density of 0.122 mW cm^{-2}. A similar situation also occurs in two types of TENG-based hydrogel electronic skin devices [265,269]. Furthermore, the conductivity, energy conversion efficiency or structural stability of some flexible materials may not be as good as rigid materials. For example, unlike rigid solar cells made from crystalline silicon, thin-film solar cells typically use lightweight semiconductor materials [22]. As a result, the reduced charge transport capacity, light absorption depth, and charge collection efficiency in thin-film solar cells lead to a decrease in their performance [24]. Therefore, the integration of the system needs to find a balance between power output and flexibility. Therefore, the integration of the system requires finding a balance between power output and flexibility. Moreover, by employing novel flexible materials (such as carbon nanotubes, graphene, etc.) [271], utilizing nanometer-scale design and surface engineering [269], and adopting reasonable structural designs (such as composite structures) [266], it is possible to enhance power output while maintaining flexibility, thus meeting practical demands.

In self-powered wearable biosensors, sensitivity and stability are

often performance metrics that limit each other. Generally, devices with high sensitivity are more susceptible to variations in environmental factors such as temperature, humidity, and mechanical stress [83,89,265,272]. However, this can lead to instability in sensor signals, as even slight changes in the environment can cause fluctuations in the sensor output. Additionally, the use of high-sensitivity materials, such as nanomaterials with a high surface area, may increase material defects or accelerate aging, which can affect the long-term performance of the device [271]. As shown in Table S3, the stability of wearable biosensors has been tested, with stability rates exceeding 90 %. However, the duration of stability testing varies, ranging from up to 5 months to only 10 cycles [89,265]. Nevertheless, it is undeniable that both high sensitivity and long-term stability are essential characteristics of an excellent wearable biosensor. Here, we summarize three strategies to balance sensitivity and stability. First, composite or functionalized material surfaces can be used. By combining high-sensitivity materials (such as MXene or graphene) with more stable matrices (such as PDMS or PVDF), the material's responsiveness and long-term durability can be balanced [272]. Second, layered or adaptive designs, along with device encapsulation, are recommended to enhance resistance to environmental interference [260]. Additionally, employing sensor arrays or signal processing methods based on machine learning can preserve the high sensitivity response while compensating for the impact of environmental changes on the signal [265].

The balance between device size and integration is also an important consideration in designing self-powered wearable biosensors. As the device size decreases, the available space becomes limited, making it increasingly difficult to add additional functional modules [103]. It leads to a reduction in integration level. Furthermore, smaller sizes can result in increased signal interference between functional units, affecting system performance. Therefore, most self-powered wearable biosensors adopt modular designs or micro/nano fabrication techniques to balance size and integration [37]. Modular design allows for functional separation, utilizing flexible connection methods to minimize space wastage [6]. Alternatively, energy harvesting and sensing functions can be integrated into a single component by developing multifunctional materials or devices, such as TENG, which can serve as both an energy harvester and a sensor [56]. Micro/nano fabrication, a more widely used approach, will be discussed in detail in the following sections.

Therefore, to balance the various performance metrics of self-powered wearable biosensors and further enhance the integration of the biosensors, we have summarized and discussed four all-in-one engineering techniques.

3.2.2. Signaling array

Signal array technology allows most biosensors, especially biophysical sensors, to integrate multiple signal units, enabling the simultaneous collection, processing, and transmission of multiple signals. Generally, the signaling arrays are integrated on soft base materials such as conductive carbon fiber [285], silicone [68,73], cotton [66], polyethylene terephthalate (PET) [8], PVDF [89], thermoplastic polyurethanes (TPU) [256], etc. [286], to achieve wearability. Furthermore, signaling array technology can integrate hundreds of units and recognize dozens of signals through planar [67,68,89], hemispherical [256], and ring-shaped sensing structures [8,66,73,166,171,273,275]. The relationship between the number of units and signal recognition is not linear. Sometimes identifying a single signal requires the participation of multiple units, while the collaboration of several units can facilitate the recognition of multiple signals [166,171,256]. For example, based on TENG and PENG self-powered technologies, a gesture recognition wristband with only 8 units can recognize 26 letters, enabling full keyboard functionality and multiple command inputs [273]. Moreover, TEG mostly uses signaling arrays to achieve up to hundreds of thermoelectric units [166,171].

However, the goal of all-in-one wearable biosensors necessitates the rational design of signaling arrays to achieve optimal signal sensing within the smallest possible effective area. As the area decreases, the issue of signal crosstalk within signaling array technology becomes increasingly severe. Here are four main strategies to mitigate this issue. Firstly, electromagnetic shielding and proper grounding are essential [264]. Using conductive materials to shield the sensitive parts of the signaling array can protect them from external electromagnetic interference. Additionally, effective grounding can reduce noise and prevent crosstalk between signal lines. Secondly, physical isolation or orthogonal routing can be employed in the structural design [270]. Increasing the physical distance between adjacent signal units (either horizontally or vertically) or routing signal lines orthogonally can minimize mutual inductance and capacitive coupling. Thirdly, employing machine learning can help identify and correct crosstalk in signal units, optimizing signal processing within the signaling array [273]. Finally, appropriately matching the impedance of the sensing circuits can minimize reflections that may cause crosstalk [287]. In general, as shown in Table 2, signal array technology focuses more on the integration of biophysical signals.

3.2.3. Microfluidic technology

Unlike signaling array technology, microfluidic technology utilizes microchannels ranging from tens to hundreds of micrometers to handle tiny volumes of fluids, focusing on the collection of biochemical energy as well as the collection and processing of biochemical signals [280,281,288]. Although only a few materials, such as PDMS and PET [61,156,196], are used as substrates, microfluidic patches can achieve precise control of fluid flow and improve the precision of chemical reactions. Most importantly, this technology requires very small volumes of biological fluids, ranging from 10^{-9} to 10^{-18} liters, providing the necessary conditions for rapid response and on-site analysis [269]. Moreover, microfluidic technology can integrate dozens of signal units, enabling parallel detection of concentrations of organic compounds and ions in biological samples [61,155,156,196,278]. Inspired by the E-BFC, a battery-free wireless electronic sensor has been developed, integrating 12 reaction units based on a timer-controlled microfluidic platform and embedded colorimetric detection [278]. In this system, the sweat glands generate pressure to drive sweat through a network of microfluidic channels and valves. These channels interface with separately placed sensors, effectively contamination and cross-talk. This platform enables the simultaneously monitoring of chloride, lactate, and glucose concentrations, as well as pH levels, sweat rate, and total sweat volume [278].

Generally, engineering strategies such as optimizing channel shapes and sizes to enhance fluid control, integrating multifunctionality into a single platform to improve system integration and scalability, and employing micromechanical structures to increase reaction efficiency, all contribute to the further advancement of microfluidic technology in wearable biosensors [61,155,156,196,278,280,281,288]. However, limited material options restrict the chemical compatibility and functionality of microfluidic technology, and it is urgent to develop new polymer materials [289]. Additionally, the complex and costly manufacturing techniques make it challenging to produce high-precision, small-sized microfluidic patches [288]. 3D printing technology can alleviate this dilemma [290]. Finally, most microfluidic sweat patches are disposable and must be encapsulated, which makes them less cost-effective and sustainable [278].

3.2.4. Screen printing

Screen printing technology involves using a stencil to transfer ink onto a substrate. Some areas of the stencil allow the ink to pass through, while other areas block the ink, resulting in a printed design. In the field of wearable biosensors, screen printing technology is commonly used not only to create structures for signal collection [148], processing [154], and transmission but also for energy harvesting and storage units [106,145,146,150,151,291]. The emergence of printable

supercapacitors has made screen printing technology even more crucial in the field of wearable biosensors [153]. Therefore, this technology utilizes a variety of printing inks, including graphene [291], carbon nanotubes [153], liquid metals [106], Au and metallic cotton fiber [145, 155]. These inks can be printed on substrates such as glass [292] , polyimide tape [293], PDMS [146] , PET [294] , textile or paper [189, 295], ensuring that wearable biosensors based on this technology are both flexible and comfortable, while also being exceptionally thin. Due to its advantages in low-cost and scalable production, screen printing technology can integrate up to hundreds of units on a single device [155, 158,189,200]. For example, He *et al.* made a fully printed planar MEG using C and C-Al as electrodes, polystyrene sulfonic acid and poly-diallyldimethylammonium chloride as reaction materials [189]. All the materials needed for this MEG can be made into screen-printed ink and printed on substrates such as clothing and PET. Through screen printing technology, they can integrate 300 MEG units, 6 supercapacitors and 1 electrochromic device into a PET sheet.

However, achieving uniform ink deposition can be challenging, leading to inconsistencies in wearable biosensor performance [296]. To this end, it is important to develop new inks with better flow properties and uniformity. Secondly, screen printing has limitations in achieving high-resolution patterns. Using finer screens and advanced emulsion technology can achieve printing needs with fine features [297]. Furthermore, there are electronic devices such as metal-oxide-semiconductor field-effect transistors (MOSFETs) that cannot be obtained through screen printing technology. Excessive stretching or bending will exceed the fracture limit, making the device extremely vulnerable to damage [297].

3.2.5. Integrated circuit

The integrated circuit, also known as a chip, is a set of electronic circuits on a small flat piece of semiconductor material. Considering wearability, the integrated circuits used in biosensors are generally based on materials such as polyimide [171], polyester film [65], epoxy resin [45,72,76,77,84], and parylene [46,83]. Unlike other integration technologies that are applied to only three parts of self-powered wearable biosensors, integrated circuits encompass all components, from energy harvesting, management, and storage to signal collection, processing, and transmission [61,65,76,77,83,84,156,171]. Especially in energy management and signal processing, the integrated circuit provides guarantees for the miniaturization, low power consumption, high performance and durability of self-powered wearable biosensors [61,65, 298]. For example, an electronic skin based on 3D integrated circuits combines electronic components with stretchable fiber substrates, liquid metal circuits, and hybrid liquid metal solders [299]. This electronic skin provides high-density complex system-level functions, creates wireless energy input, and also covers the analysis and processing of biological signals as well as communication. Song *et al.* integrated the TENG in independent layer working mode, sweat sensor patch and wireless sensor circuit on a soft printed circuit board platform to achieve in-situ monitoring of biomarkers in the wearer's sweat [61]. They found that the design and preparation of the sweat sensor system are compatible with the traditional manufacturing process of flexible printed circuit boards, so it can be further mass-produced and highly integrated.

However, due to limitations in substrate materials, soldering materials, and rigid electronic components, the flexibility of integrated circuits still needs improvement [300]. Moreover, the complex manufacturing techniques and high production costs of integrated circuits often deter researchers from pursuing their development. Most importantly, a large number of compact electronic components cause integrated circuits to generate heat during operation [301]. Therefore, efficient heat dissipation becomes an urgent problem to be solved when wearable biosensors use integrated circuits. Furthermore, the electromagnetic interference caused by integrated circuits further impacts the sensing performance and accuracy of wearable biosensors [302].

4. Communication technologies for all-in-one wearable biosensor systems

Either for precise medical treatment or personalized monitoring, communication between wearable biosensors and users is essential. This interaction helps doctors provide timely medical interventions and enables users to adjust their behavior promptly. Generally, commercial sensors come with built-in communication capabilities. Only active biosensors need to be paired with suitable signal transmission technologies based on their power supply conditions. According to statistics, self-powered biosensors prefer signal transmission technologies that consume power in the range of 0.01–130 mW, which is marked in Fig. 1**B**, Table 3 and Table S4. Apart from energy consumption, self-powered biosensors also consider factors such as size, transmission distance, and wearability when selecting signal transmission technologies to meet integration requirements (Table 3). Furthermore, we analyze the limitations of each signal transmission technology, present the state-of-the-art transmission technologies and methods in the field, and highlight the challenges that need to be addressed for continued development.

4.1. Radio frequency communication technology

Radio frequency (RF) communication technology refers to the use of electromagnetic waves with frequencies between 3 kHz and 300 GHz to transmit and receive signal data, which is crucial in wireless communication technology. RF technology encompasses both near-field and far-field communication techniques. Near-field communication technology generally operates at lower frequencies, usually below 30 MHz, with common applications using frequencies around 125 kHz and 13.56 MHz [8,65,77,115–117,280,281]. The signal transmission distance of near-field communication technology ranges from a few centimeters to a few meters. Far-field communication technology operates at higher frequencies, typically ranging from a few hundred MHz to several GHz, enabling long-range communication and supporting high data rates.

However, due to limitations (such as transmitter power, antenna design, and environmental conditions), the signal transmission distance of RF communication technologies is typically restricted to within 2000 centimeters in the field of self-powered wearable biosensors, and the operating frequency is usually 1 kHz-1000 MHz [8,48,69,73,77,84,115, 116,118,119,278]. By receiving 250 Hz and 1 kHz radio waves, a TENG-based self-powered hybrid encoder can transmit Morse code and Gray code to send text messages or remotely control electronic devices by encoding two actions: touch and press, with a maximum communication distance of about 2000 cm [77]. Furthermore, these RF communication technologies range in overall size from 1 to 50 cm^2 and consume energy from 0.01 to 20 mW [8,65,69,84,106,115–117,280, 281]. To miniaturize the pacemaker platform, an RF device with a total area of about 0.99 cm^2 for the receiver and control unit was tested in vitro and in vivo, and could transmit signals over a distance of 25 cm [115]. In order to send temperature data to a mobile phone at a transmission frequency of 1 Hz, the overall power consumption of the microcontroller unit of a self-powered integrated microsystem can be as high as 15 mW [98]. Furthermore, RF backscatter has recently become a low-cost technology, consuming only μW of power [48]. Based on ultra-thin flexible circuits and microcontroller chips, RF communication technology (433 MHz) enables a smart contact lens to perform real-time electrochemical biosensing and on-demand controlled drug delivery, with a communication distance of 5 cm and a power consumption of only 2.3 mW [118]. Therefore, the wearability of RF communication technology relies on the use of liquid metals like magnesium and tungsten, as well as flexible electrodes like copper, and substrates such as PLGA, PDMS, PVC, parylene, and polyimide [8,69,106,115,116,118]. However, RF communication technologies across various frequency bands rely on custom chips or different commercial transmitters, making

Table 3
Comparison of communication technologies for all-in-one self-powered wearable biosensor systems.

Technologies	RF communication technology (1 kHz-1000 MHz)	Bluetooth communication (2.4 GHz)	Wi-Fi (2.4 GHz)	Visual display
Size	1–50 square centimeters	1–20 square centimeters	-	0.09–100 square centimeters
Power consumption	0.01–20 milliwatts	0.05–130 milliwatts	0.04–0.07 milliwatts (for passive Wi-Fi), 50–330 milliwatts (for Wi-Fi)	0.01–45 milliwatts
Transmission distance	Within 2000 centimeters	Within 100 centimeters	Within 3000 centimeters	-
Softness	With flexible coils and substrates, soft devices can be made	With flexible substrates, soft devices can be made	Only hard signal transmission module	With flexible coils and substrates, soft devices can be made
Ref.	[8,48,65,69,73,77,84,98,106,115–119, 278,280,281,303]	[48,61,66,98,171,176,181,259, 304,305]	[35,38,48,306,307]	[33,40,67,127,189,283,308]

it challenging to establish connectivity with personal user devices like smartphones. Additionally, the rise of Long Range and Narrowband IoT communication technologies offers an alternative perspective for long-distance, low-power signal transmission [303].

4.2. Bluetooth communication

As one of the far-field communication technologies, Bluetooth uses radio waves in the 2.400–2.485 GHz frequency band to create a highly secure personal area network for communication. In the field of self-powered wearables, Bluetooth communication is favored due to its user-friendly interface, simple pairing process and strong compatibility. Based on mature module manufacturing technology, the size of the Bluetooth module used in the self-powered wearable biosensor is 1–20 cm^2, and the data transmission distance is about 100 cm [171,259]. It is worth noting that the signal transmission distance mentioned here is the longest distance used in the examples [48,61,66,98,181,304]. In fact, with sufficient power supply and unobstructed space, Bluetooth usually supports a communication range of up to 1000 cm. Generally, the energy consumed by Bluetooth signal transmission is relatively low [48,61, 98,181,304], and a commercial module consumes as little as 0.043 mW [176]. However, the Bluetooth module consumes a lot of energy at the moment of connection [66], so its average energy consumption may be as high as 130 mW [259]. Moreover, research on making flexible Bluetooth communication modules is still ongoing [305].

4.3. Wi-Fi

Wi-Fi is the abbreviation of Wireless Fidelity and is also a far-field communication technology (frequency, 2.4 GHz). Similar to Bluetooth communication technology, it is often used by self-powered wearable biosensors to transmit signals with personal terminals. Due to the need to continuously transmit and receive data using radio frequency signals, the energy consumed by Wi-Fi communication technology in the field of self-powered wearable biosensors ranges from 50 to 330 mW [38,48]. Recently, passive Wi-Fi has attracted attention for wearable biosensors due to significantly reduced power consumption [35]. In a passive Wi-Fi system, the master device actively generates and sends radio frequency signals, and the sensors reflect these signals with minimal power, encoding their data in the process. Kellogg *et al.* demonstrated that smartphones and Wi-Fi chipsets can decode passive Wi-Fi for data transmission within 100 feet in both line-of-sight and through-wall scenarios [306]. They designed a passive Wi-Fi integrated circuit capable of transmitting signals at rates of 1 Mbps and 11 Mbps, consuming only 14.5 μW and 59.2 μW, respectively. This represents a power consumption 10000 times lower than existing Wi-Fi chipsets and 1000 times lower than Bluetooth. However, passive Wi-Fi supports transmission of lower data rates and smaller amounts of data. Moreover, Wi-Fi communication technology can transmit signals up to 3000 cm, while passive Wi-Fi has a relatively short communication distance and exhibits higher latency [306,307].

Overall, whether using far-field communication technologies like Bluetooth and Wi-Fi or near-field communication technologies, they are susceptible to interference from other electronic devices, atmospheric conditions, and physical obstacles. Additionally, security vulnerabilities such as eavesdropping are critical concerns for wearable biosensors employing these communication technologies.

4.4. Visual display

For precise personal monitoring, lag-free visual display provides a more intuitive user experience. Self-powered wearable biosensors use LEDs or simple display devices composed of LEDs for low-power signal transmission. For example, a freely constructible self-powered visual tactile sensor composed of TENG and LEDs can realize the visual perception of the palm grasping state and force feedback [67]. Additionally, electrochromic screens and electronic ink displays are employed for direct visual signal transmission, with power consumption ranging from 0.01 to 45 mW [33,40,127,308]. Among them, the electronic ink screen has the advantages of stable display, ultra-low power consumption, high contrast, etc. A self-powered smart watch based on the electronic ink screen realizes real-time signal processing, sensing and display of sweat glucose level [33]. More importantly, the electrochromic-based signal transmission technology enables visual displays to be directly applied to contact lenses, achieving non-invasive glucose sensing [283]. In this smart contact lens, the area of each electrode unit involved in reaction and color display is about 0.096 cm^2. Therefore, according to statistics [33,67,189,283], the size of devices for visual display ranges from 0.09 to 100 cm^2. Furthermore, with the use of flexible substrates like PDMS, visual display devices offer enhanced wearability [283].

5. Fully all-in-one self-powered wearable biosensor systems

Although many self-powered wearable biosensors have been reported, most of them are active biosensors as we introduced above. These active biosensors still require the support of external power to perform subsequent data collection, processing and transmission. Therefore, the ideal all-in-one self-powered wearable biosensor system would combine energy harvesting, management, and storage capabilities, allowing for autonomous signal collection, processing, and transmission, as shown in Fig. 5**A**. Moreover, the all-in-one systems draw energy from the wearers' body and their surrounding environment, enabling a wireless, miniaturized, flexible, and multifunctional wearable experience. However, the overall system has multiple complex components, and the various electrical engineering between the components is challenging. By efficiently allocating energy within the system and meticulously designing signal-sensing components, the all-in-one self-powered sensors have achieved biosensing capabilities that range from external to internal body monitoring, and from rigid devices to flexible patches. The following four examples demonstrate the components and functions of the fully all-in-one self-powered wearable

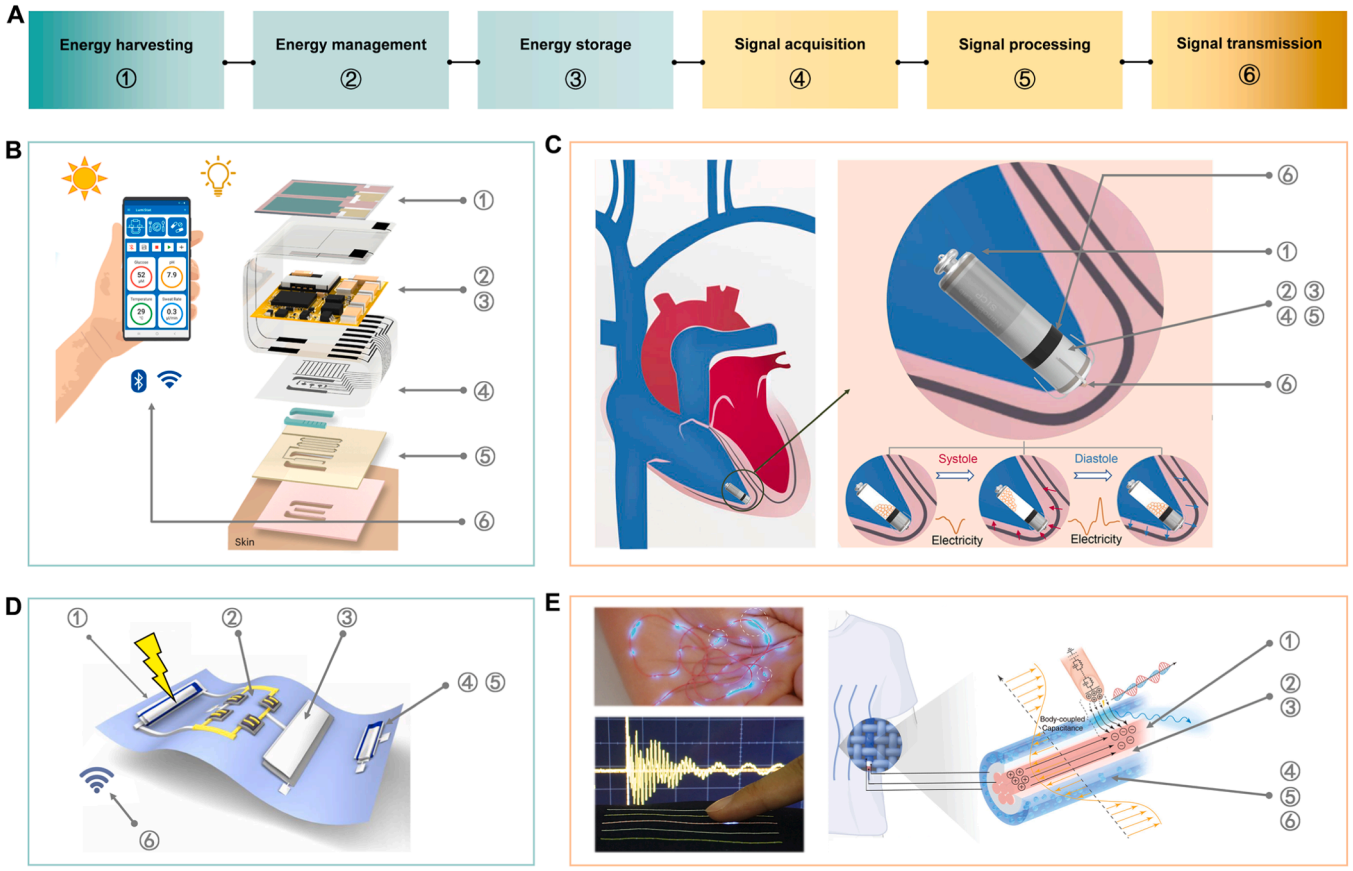

Fig. 5. Fully all-in-one self-powered wearable biosensor systems. (A) Six components of the all-in-one self-powered wearable biosensor system. (B-E) Four examples of all-in-one self-powered wearable biosensor systems. (B) An autonomous wearable biosensor powered by perovskite SCs provides continuous and noninvasive metabolic monitoring. (C) An intracardiac pacemaker based on TENG. (D) A wireless electronic health patch for monitoring pulse and measuring blood pressure based on PENGs. (E) A chip-free single optical fiber based on body-coupled energy interaction mechanism for realizing wireless visual-digital interaction. Panels

Reproduced with permission from: (B) ref. 37, Springer Nature Ltd.; (C) ref. 72, Springer Nature Ltd.; (D) ref. 83, Springer Nature Ltd.; (E) ref. 316, the American Association for the Advancement of Science.

biosensor systems, covering the sensing of biochemical and biophysical signals.

5.1. *Biomarker monitoring*

The content of glucose and various ions in body fluids provides physiologically and metabolically rich information for personal disease diagnosis and health monitoring. Notably, self-powered sweat detection patches applied to the skin are highly valued in the wearable biosensor field due to their non-invasive, in-situ, and autonomous sensing advantages. As shown in Fig. 5**B**, the self-powered wearable sweat detection patch covers all components of the all-in-one system. The initial integrated wearable sweat patches did not achieve self-powering functionality [241]. However, they combined plastic sensors with silicon integrated circuits for signal acquisition and complex signal processing, enabling the sensing of sweat metabolites, electrolytes, and skin temperature. In the signal collection and processing module, the body's sweat glands provide pressure to force sweat through microfluidic channels and valves connected to separately placed sensor interfaces [278]. Compared with commercial glucose sensors that rely on microneedles that pierce the skin, sweat patches based on microfluidic platforms minimize skin irritation and signal source contamination and crosstalk. Therefore, leveraging a timed microfluidic platform, embedded colorimetric assay, and near-field communication technology, a BFC-inspired biosensing platform achieves all-in-one battery-free wireless sweat signal sensing, which has the advantages of being lighter, cheaper, and smaller than alternatives [278]. Although NFC can support continuous communication, it is typically used for intermittent, low-power exchanges. Therefore, novel energy harvesting devices such as WPT-EF, E-BFC, TENGs, SCs, and HGs have been incorporated into sweat patches, enabling self-powered functionality [37,61,156,207]. For instance, an autonomous wearable sweat sensor utilizes flexible perovskite SCs (PCE, ~31.2 %) and a flexible printed circuit board for energy harvesting (①), management (②), and storage (③) (Fig. 5**B**) [37]. It employs iontophoresis and dynamic microfluidics to extract and collect sweat signals (④), and uses various electrochemical detection techniques for multi-channel monitoring of biological signals in sweat (⑤) [37]. Finally, it leverages Bluetooth for communication between the sensor and a smartphone (⑥). The device dimensions of the fully all-in-one wearable biosensor mentioned above are 2 cm× 2.7 cm× 0.4 cm and can be comfortably adhered to the skin, truly realizing the continuous collection of multimodal physical and chemical signals.

Moreover, utilizing WPT-EF and E-BFC energy harvesting technologies, smart contact lenses can integrate flexible circuit boards, glucose sensors, and flexible transparent antennas to monitor glucose concentration in tears [118,283,309]. It also represents a typical design of the all-in-one self-powered wearable biosensor system, offering promising real-time, non-invasive monitoring and diagnosis for diabetic patients. Additionally, self-powered wearable biosensor systems based on biological fluids such as saliva and urine are also steadily advancing toward an era of full integration [158,310].

5.2. Implantable biosensing devices

Researchers have been pursuing the integration of self-powered biosensors in vivo, such as pacemakers and deep brain stimulation devices. The reasons are as follows. Firstly, traditional implantable devices may cause circuit breakage and inevitable skin scarring during implantation [311]. Although wireless implantable devices with batteries address some of the above complications, battery capacity limitations make long-term operation of the devices challenging [312]. Therefore, it is highly desirable for implantable biosensors to possess both self-powered capabilities and fully all-in-one devices. For example, by utilizing TENG to harvest mechanical motion energy from cardiac motion, a capsule-structured pacemaker (1.75 g, 1.52 cc) integrates an energy harvesting unit (①), an energy management and storage unit (②③), and a pacemaker module (④⑤⑥), as shown in **Figure 5 C** [72]. The effectiveness and safety of the pacemaker have been demonstrated in a large animal cardiac pacing model, laying a solid foundation for the application of fully all-in-one self-powered pacemakers in humans. Furthermore, powered by resonant inductive coupling technology based on WPC-EF, temporary cardiac pacemakers can control heart rate and rhythm post-surgery [116]. Made from bioabsorbable materials, these pacemakers fully dissolve and are naturally cleared from the body within the specified surgical period, forming the foundation for the next generation of postoperative temporary pacing technology.

Another highly integrable in vivo biosensing device is the wireless neural stimulator [115,123,124]. Based on the magnetoelectric materials, the neural stimulator can be used for deep brain stimulation and miniaturized to a millimeter scale [123]. Its implantable component can be simplified to include only a magnetoelectric material, a diode, and an LED [122]. This wireless neural stimulator's emphasis on self-powering capabilities and integrated design allows for minimally invasive and long-lasting interfaces with brain regions and peripheral nerves. However, as the stimulator becomes more integrated and miniaturized, ensuring the safety of the human body and the stability of the device's operation during energy supply becomes increasingly critical [313].

5.3. Wireless electronic health patches

Apart from some mechanical sensors used for joint and skeletal rehabilitation that require rigid components [93,167], the ideal model for most wearable biosensors is the wireless electronic health patch. Most biomarker monitoring is based on the electronic patch, which has been introduced above. For monitoring biophysical signals, mature electronic sensors have addressed the issues of signal collection, processing, and transmission. Therefore, the obstacles to full integration are primarily focused on the units responsible for energy harvesting, management, and storage. However, in the early research of wireless electronic health patches, solid electronic components and substrate materials that are not conformal to the skin make biological individuals have a poor wearing experience [165]. The latest generation of wireless electronic health patches utilizes flexible energy harvesters such as TENG, PENG, and WPT-EF [83,202]. These patches also incorporate flexible energy management components like organic diodes and flexible energy storage elements such as printable supercapacitors, achieving outstanding flexibility. For example, as illustrated in Fig. 5**D**, an ultra-flexible wireless electronic health patch integrates PENG (①), organic semiconductor diodes (②), and thin-film capacitors (③), with each component having a thickness of no more than 2.5 μm [83]. Based on a 1 μm-thin parylene substrate, this patch combines the PENG-based active biophysical sensor (④⑤) and the wireless signal transmission device (⑥) to measure pulse and blood pressure unobtrusively. Moreover, utilizing a normalized fabric circuit board quasi-surface mount technology, a hybrid energy harvesting system seamlessly integrates a wearable rectifying antenna, TENG, and PMC into a single fabric substrate, resulting in a fabric-based wireless electronic health patch [202]. Furthermore, the mechanical incompatibility between soft surface devices and rigid high-performance silicon electronic devices can be solved by integrating RFID technology with flexible readout circuits [314].

Most importantly, the development of wireless electronic health patches must also focus on efficient, user-friendly, large-scale production technology. Therefore, technologies such as screen printing, inkjet printing integrated processes, and 3D printing are used to lay the foundation for the mass production of wireless electronic health patches [139,189].

5.4. Smart textile electronics

In self-powered wearable biosensors, flexible and breathable smart textile electronics offer the most comfortable means for daily biochemical and biophysical monitoring of individuals. Early self-powered wearable biosensors merely stitch various components onto textile substrates or fashion polymer fibers and similar materials into energy harvesters to power different electronic sensors [204,261]. For example, a hybrid textile based on lightweight polymer fibers can simultaneously harvest energy from ambient sunlight and mechanical movement to power electronic watches, etc [203]. However, they still rely on rigid electronic components and are less integrated than flexible electronic patches. With advancements in energy harvesting technology, electroluminescence, and optical fiber technology, smart textile electronics have demonstrated increasingly innovative methods for biosensing. Based on textile engineering and fiber electronics technology, an intelligent textile lighting/display system integrates multiple functions, realizing wireless power transmission and energy storage, as well as monitoring and transmission of biological signals [315]. As shown in Fig. 5**E**, an optical fiber electronic technology that uses the interaction object itself to couple ambient electromagnetic energy has enabled wireless energy harvesting, wireless signal transmission, and direct signal display [316]. Optical fiber cores made from silver-plated nylon fibers are used to induce alternating electromagnetic fields for energy harvesting (①). The dielectric layer stores the collected energy (②③), while the optical layer is employed for sensing and direct visual display (④⑤⑥). This smart textile electronics demonstrates a self-powered, seamlessly integrated chip-free system, which adds more possibilities for energy collection and signal transmission of wearable biosensors.

6. Summary and outlook

All-in-one self-powered wearable biosensors offer an in-situ sensing solution that is ready-to-use, battery-free, and wireless, enabling precise medical diagnostics and personalized monitoring. A diverse array of energy harvesting, management, and storage strategies, combined with precise methods for signal acquisition, processing, and transmission, provides a comprehensive toolbox for developing the next generation of biosensors. These biosensors will achieve system-level integration and miniaturization while maintaining wearability and durability. Although these all-in-one biosensors are promising, engineering issues arising from the integration and connection of the six modules still exist. Mastering the energy conversion and signal acquisition processes at various stages within an all-in-one platform not only requires enhancing the performance of each module but also demands advancements in materials engineering, device design, and intelligent algorithms. Yet, to fully realize the potential of all-in-one self-powered wearable biosensors, there are still numerous challenges and emerging technologies for development within the six modules. These include self-consistent design and biodegradable technologies, efficient hybrid energy harvesting technologies, flexible chip technologies, flexible batteries and supercapacitors, synchronous signal acquisition and high-frequency sampling technologies, wearable bio-inspired designs, on-chip computation and analysis technologies, cloud-edge collaborative signal processing technologies, AI-assisted signal processing technologies, and 5 G and 6 G communication technologies. Specific prospects are as follows:

Energy harvesting (Fig. 6**A**). When selecting the appropriate power strategy for all-in-one wearable biosensors, the primary consideration should be the self-consistency between the energy harvester and the application scenario. Self-consistency not only refers to the power matching between self-power technology and sensing applications, but also refers to the fit of the working environment of the two. For example, it is more reasonable for smart contact lenses to use MEG and E-BFC for power supply than WPT-EF technology. The moisture and certain metabolites in tears serve as energy sources for MEG and E-BFC, which supports a more streamlined and integrated design. Moreover, the heart's rhythmic beating causes periodic deformation of materials attached to it. Therefore, designing cardiac pacemakers based on TENG and PENG technologies is more logical. Secondly, the degradability of materials should not only be a consideration for energy harvesters but also a criterion for entering the all-in-one biosensor material library. For external wear, biodegradable biosensors are more environmentally friendly. For in vivo implants, biosensors that act as temporary treatment devices are more user-friendly if they degrade or dissolve under specific triggering conditions [116]. Lastly, since most energy harvesting modules occupy the main space of all-in-one biosensors, the development of efficient hybrid energy harvesting technologies is essential to improve energy output, extend operating conditions, and enhance reliability. And the materials should have high wearability, including properties such as breathability and non-toxicity.

Energy management and energy storage (Fig. 6**B**, and Fig. 6**C**). Currently, energy management in all-in-one biosensors faces two major challenges: flexibility and miniaturization. The flexibility of electronic components significantly enhances the wearability of integrated biosensors. Miniaturization not only brings size advantages but also reduces the energy demand. Flexible chip technology, which is in the early stages of research, may meet these requirements. Among them, the research and development of thin-film field-effect transistors, two-dimensional semiconductor transistors and carbon-based chips are expected to achieve highly integrated, low-power and high-conversion energy management modules [317–319]. Similarly, energy storage also faces the problem of flexibility. Flexible batteries and supercapacitors are effective ways to solve the above problems. Graphene-based supercapacitors and MXene-based micro--supercapacitors, with their high flexibility, thin profiles, and excellent performance, are likely to become the preferred energy storage devices for the next generation of all-in-one biosensors [320].

Signal acquisition (Fig. 6**D**). The next generation of all-in-one wearable biosensors will focus primarily on the synchronized acquisition of multi-mode signals and high-frequency sampling. On the one hand, a wearable biosensor system uses signal arrays or microfluidics technology to simultaneously collect multiple signals from the organism, which not only improves the integration of the system but also reduces energy consumption by reducing the number of sensors. On the other hand, improving the sampling frequency of the all-in-one biosensor system can accurately reflect the detailed information of important biological signals. For example, the original signals of human heart rate and pulse contain rich information that can reflect physical health. A high sampling rate can restore the current physical condition as much as possible, laying the foundation for preventing various diseases. Additionally, leveraging bio-inspired structures to collect biological signals, thereby enhancing the performance, comfort, and durability of wearable devices, is also crucial [242]. For example, microfluidic designs mimicking the vascular system can be used to achieve efficient transport of biological fluids.

Signal processing (Fig. 6**E**). To enhance processing efficiency and enable in-situ processing, the development of on-chip computing and analysis, as well as cloud-edge collaborative signal processing methods, is inevitable. For the all-in-one wearable biosensor, real-time computing and analysis on the built-in chip greatly improve the efficiency of instant

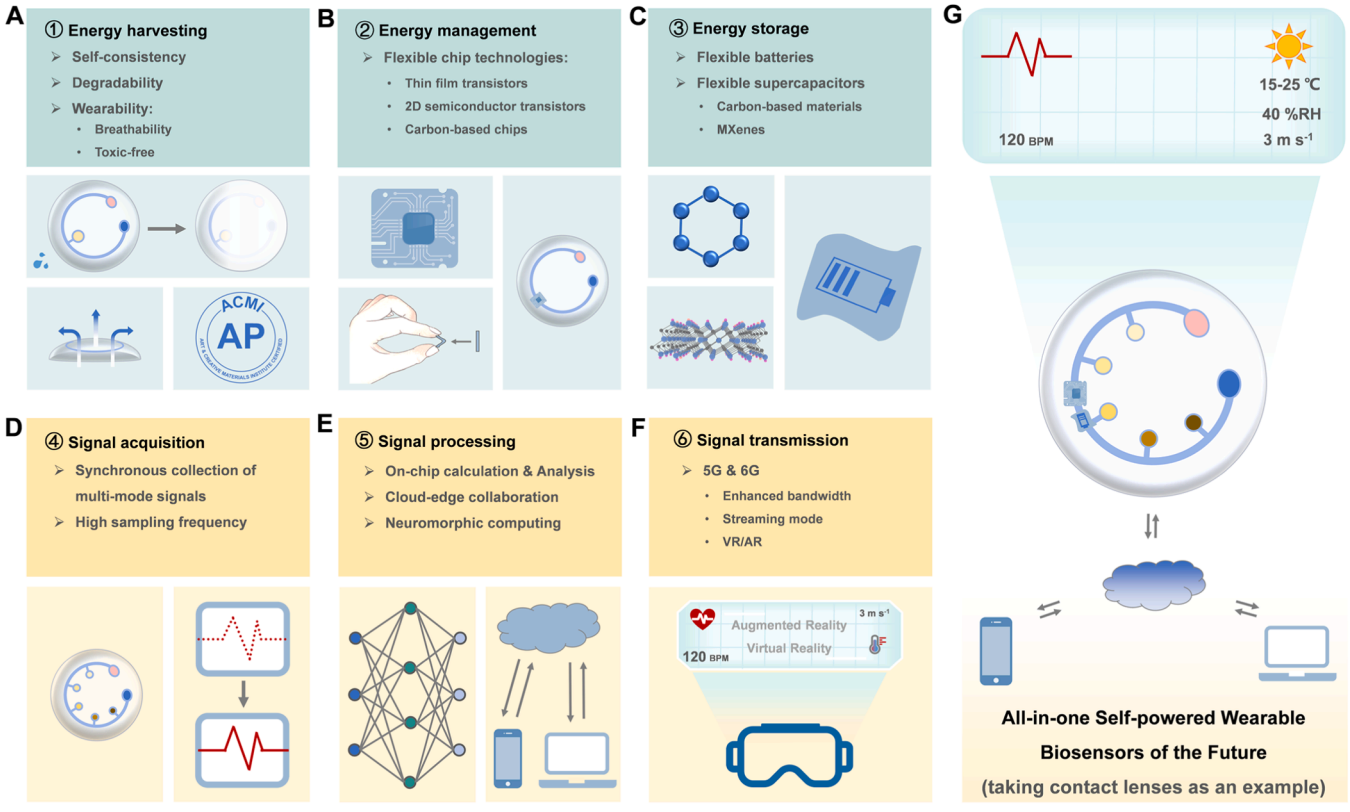

Fig. 6. Outlook of the all-in-one self-powered wearable biosensor system. Taking contact lenses as an example, wearable biosensor systems will gradually enhance the performance of six major components in the future, truly achieving wearability, self-powering, and integration. 5 G, 5th generation mobile communication technology. 6 G, 6th generation mobile communication technology. VR, virtual reality. AR, augmented reality. BPM, beat per minute. RH, relative humidity.

diagnosis of individual physical conditions, which is particularly important for precision medicine for patients. Additionally, biosensors can transmit large and complex signal data to public servers, enabling collaborative cloud and edge computing to maximize data value. For instance, wearers share the temperature and humidity of the nearby environment. Moreover, the entire signal processing process can be optimized with the help of artificial intelligence algorithms. For example, by simulating the neural structure and function of the human brain, neuromorphic computing can simultaneously acquire and process biological signals, with high energy efficiency, fast parallel processing speed, and strong scalability [321]. It can form a multi-sensory neural network and is a potential signal-processing strategy for future all-in-one wearable biosensors [322].

Signal transmission (Fig. 6**F**). With the development of wearable biosensors, the transmission methods of signals will be more diverse in the future. Most importantly, the bandwidth for signal transmission should be enhanced, with better support for streaming modes, which is the key to 5 G and 6 G communication technologies. The 5 G and 6 G communication technologies signify true real-time signal transmission. It means that wearable biosensors based on these technologies can act as mediums for real-time human-computer interaction, enabling the possibilities of virtual reality and augmented reality. Last but not least, the design of all-in-one self-powered wearable biosensors should take into account both the wearer's physical safety and information security, from energy collection to signal transmission.

In the foreseeable future, energy harvesting, management and storage, as well as signal acquisition, processing and transmission, will achieve a qualitative leap. The all-in-one self-powered wearable biosensors will be the culmination of all. As shown in Fig. 6**G**, a small smart contact lens will collect most of the wearer's external, surface and internal signals and display them in front of the wearer in the form of mixed reality.

CRediT authorship contribution statement

Cheng Wenlong: Writing – review & editing. **Xi Yi:** Writing – review & editing, Visualization, Supervision, Funding acquisition, Data curation. **Chu Dewei:** Writing – review & editing, Visualization. **Lu Yuerui:** Writing – review & editing, Visualization, Supervision, Funding acquisition, Conceptualization. **Sun Xueqian:** Writing – review & editing. **Gao Mingyuan:** Writing – review & editing, Visualization, Formal analysis, Data curation. **Wang Xiaolin:** Writing – review & editing, Data curation. **Li Qianying:** Writing – review & editing, Writing – original draft, Investigation, Formal analysis, Data curation.

Declaration of Competing Interest

The authors declare that they have no known competing financial interests or personal relationships that could have appeared to influence the work reported in this paper.

Acknowledgements

Q.L. thanks to the China Scholarship Council for awarding State Scholarship Fund (csc202306050075). This work was supported by the National Natural Science Foundation of China (NSFC) (52272191 and 52008343) and the National Key R & D Project from Minister of Science and Technology (2021YFA1201602). Y. L. acknowledges funding support from the Australian Research Council (grant no: DP240101011) and the National Health and Medical Research Council (NHMRC; ID: GA275784).

Appendix A. Supporting information

Supplementary data associated with this article can be found in the online version at doi:10.1016/j.mser.2025.100934.

Data availability

No data was used for the research described in the article.

References

[1] J. Wu, H. Liu, W. Chen, B. Ma, H. Ju, Device integration of electrochemical biosensors, Nat. Rev. Bioeng. 1 (2023) 346–360.
[2] L.C. Clark, C. Lyons, Electrode systems for continuous monitoring in cardiovascular surgery, Ann. N. Y. Acad. Sci. 102 (1962) 29–45.
[3] H.C. Ates, et al., End-to-end design of wearable sensors, Nat. Rev. Mater. 7 (2022) 887–907.
[4] Q.H. Shu, et al., Flexible resistive tactile pressure sensors, J. Mater. Chem. A 12 (2024) 9296–9321.
[5] Y.H. Chen, et al., Skin-like biosensor system via electrochemical channels for noninvasive blood glucose monitoring, Sci. Adv. 3 (2017) e1701629.
[6] V. Nair, et al., Miniature battery-free bioelectronics, Science 382 (2023) eabn4732.
[7] R.Y. Liu, Z.L. Wang, K. Fukuda, T. Someya, Flexible self-charging power sources, Nat. Rev. Mater. 7 (2022) 870–886.
[8] F. Liu, et al., Self-powered wireless body area network for multi-joint movements monitoring based on contact-separation direct current triboelectric nanogenerators, Infomat 5 (2023) e12428.
[9] W. Kim, et al., Magnetoelectrics enables large power delivery to mm-sized wireless bioelectronics, J. Appl. Phys. 134 (2023) 094103.
[10] A.E. Ostfeld, A.M. Gaikwad, Y. Khan, A.C. Arias, High-performance flexible energy storage and harvesting system for wearable electronics, Sci. Rep. 6 (2016) 26122.
[11] H. Lee, et al., Toward all-day wearable health monitoring: An ultralow-power, reflective organic pulse oximetry sensing patch, Sci. Adv. 4 (2018) eaas9530.
[12] X.J. Pu, et al., Eye motion triggered self-powered mechnosensational communication system using triboelectric nanogenerator, Sci. Adv. 3 (2017) e1700694.
[13] C.A. Gueymard, A reevaluation of the solar constant based on a 42-year total solar irradiance time series and a reconciliation of spaceborne observations, Sol. Energy 168 (2018) 2–9.
[14] D.M. Chapin, C.S. Fuller, G.L. Pearson, A new silicon P-N junction photocell for converting solar radiation into electrical power, J. Appl. Phys. 25 (1954) 676–677.
[15] D. Sharma, R. Mehra, B. Raj, Comparative analysis of photovoltaic technologies for high efficiency solar cell design, Superlattices Microstruct. 153 (2021) 106861.
[16] A.S. Al-Ezzi, M.N.M. Ansari, Photovoltaic solar cells: A Review, Appl. Syst. Innov. 5 (2022) 67.
[17] P. Roy, N.K. Sinha, S. Tiwari, A. Khare, A review on perovskite solar cells: Evolution of architecture, fabrication techniques, commercialization issues and status, Sol. Energy 198 (2020) 665–688.
[18] B. Min, et al., A roadmap toward 24% efficient PERC solar cells in industrial mass production, IEEE J. Photovolt. 7 (2017) 1541–1550.
[19] K. Yoshikawa, et al., Silicon heterojunction solar cell with interdigitated back contacts for a photoconversion efficiency over 26%, Nat. Energy 2 (2017) 17032.
[20] H. Lin, et al., Silicon heterojunction solar cells with up to 26.81% efficiency achieved by electrically optimized nanocrystalline-silicon hole contact layers, Nat. Energy 8 (2023) 789–799.
[21] X.Z. Wu, High-efficiency polycrystalline CdTe thin-film solar cells, Sol. Energy 77 (2004) 803–814.
[22] J. Ramanujam, et al., Flexible CIGS, CdTe and a-Si:H based thin film solar cells: A review, Prog. Mater. Sci. 110 (2020) 100619.
[23] D.B. Li, et al., 20%-efficient polycrystalline Cd(Se,Te) thin-film solar cells with compositional gradient near the front junction, Nat. Commun. 13 (2022) 7849.
[24] J. Zhou, et al., Highly efficient and stable perovskite solar cells via a multifunctional hole transporting material, Joule 8 (2024) 1691–1706.
[25] W. Li, et al., The critical role of composition-dependent intragrain planar defects in the performance of $MA_{1-x}FA_xPbI_3$ perovskite solar cells, Nat. Energy 6 (2021) 624–632.
[26] I. Mathews, S.N. Kantareddy, T. Buonassisi, I.M. Peters, Technology and market perspective for indoor photovoltaic cells, Joule 3 (2019) 1415–1426.
[27] J. Dagar, S. Castro-Hermosa, G. Lucarelli, F. Cacialli, T.M. Brown, Highly efficient perovskite solar cells for light harvesting under indoor illumination via solution processed SnO_2/MgO composite electron transport layers, Nano Energy 49 (2018) 290–299.
[28] M. Li, et al., Interface modification by ionic liquid: a promising candidate for indoor light harvesting and stability improvement of planar perovskite solar cells, Adv. Energy Mater. 8 (2018) 1801509.
[29] A.S. Teran, et al., AlGaAs photovoltaics for indoor energy harvesting in mm-scale wireless sensor nodes, IEEE Trans. Electron Devices 62 (2015) 2170–2175.
[30] M. Rani, et al., Breaking barriers: Addressing challenges in perovskite solar cell development, J. Alloy. Compd. 1010 (2025) 177648.
[31] A. Kojima, K. Teshima, Y. Shirai, T. Miyasaka, Organometal halide perovskites as visible-light sensitizers for photovoltaic cells, J. Am. Chem. Soc. 131 (2009) 6050–6051.
[32] K.L. Gardner, et al., Nonhazardous solvent systems for processing perovskite photovoltaics, Adv. Energy Mater. 6 (2016) 1600386.

[33] J.Q. Zhao, et al., A fully integrated and self-powered smartwatch for continuous sweat glucose monitoring, Acs Sens 4 (2019) 1925–1933.
[34] C. Li, et al., Flexible perovskite solar cell-driven photo-rechargeable lithium-ion capacitor for self-powered wearable strain sensors, Nano Energy 60 (2019) 247–256.
[35] S. Castro-Hermosa, et al., Perovskite photovoltaics on roll-to-roll coated ultra-thin glass as flexible high-efficiency indoor power generators, Cell Rep. Phys. Sci. 1 (2020) 100045.
[36] S. Kim, et al., High-power and flexible indoor solar cells via controlled growth of perovskite using a greener antisolvent, ACS Appl. Energy Mater. 3 (2020) 6995–7003.
[37] J.H. Min, et al., An autonomous wearable biosensor powered by a perovskite solar cell, Nat. Electron. 6 (2023) 630–641.
[38] A.S. Khan, F.U. Khan, A wearable solar energy harvesting based jacket with maximum power point tracking for vital health monitoring systems, IEEE Access 10 (2022) 119475–119495.
[39] N. Piva, et al., Tattoo-like transferable hole selective electrodes for highly efficient, solution-processed organic indoor photovoltaics, Adv. Electron. Mater. 4 (2018) 1700325.
[40] D. Landerer, et al., Solar glasses: a case study on semitransparent organic solar cells for self-powered, smart, wearable devices, Energy Technol. 5 (2017) 1936–1945.
[41] W.Y. Jin, M.M. Ovhal, H.B. Lee, B. Tyagi, J.W. Kang, Scalable, All-printed photocapacitor fibers and modules based on metal-embedded flexible transparent conductive electrodes for self-charging wearable applications, Adv. Energy Mater. 11 (2021) 2003509.
[42] S. Park, et al., Self-powered ultra-flexible electronics via nano-grating-patterned organic photovoltaics, Nature 561 (2018) 516–521.
[43] M.C. Tsai, et al., A large, ultra-black, efficient and cost-effective dye-sensitized solar module approaching 12% overall efficiency under 1000 lux indoor light, J. Mater. Chem. A 6 (2018) 1995–2003.
[44] M. Freitag, et al., Dye-sensitized solar cells for efficient power generation under ambient lighting, Nat. Photon 11 (2017) 372–378.
[45] K. Song, et al., Subdermal flexible solar cell arrays for powering medical electronic implants, Adv. Healthc. Mater. 5 (2016) 1572–1580.
[46] Y. Nam, et al., Ultra-thin GaAs single-junction solar cells for self-powered skin-compatible electrocardiogram sensors, Small Methods 8 (2024) 2301735.
[47] C.C. Wu, et al., $FAPbI_3$ flexible solar cells with a record efficiency of 19.38% fabricated in air via ligand and additive synergetic process, Adv. Funct. Mater. 29 (2019) 1902974.
[48] I. Mathews, et al., Self-powered sensors enabled by wide-bandgap perovskite indoor photovoltaic cells, Adv. Funct. Mater. 29 (2019) 1904072.
[49] Y.M. Cao, Y.H. Liu, S.M. Zakeeruddin, A. Hagfeldt, M. Grätzel, Direct contact of selective charge extraction layers enables high-efficiency molecular photovoltaics, Joule 2 (2018) 1108–1117.
[50] W.Z. Liu, et al., Flexible solar cells based on foldable silicon wafers with blunted edges, Nature 617 (2023) 717–723.
[51] Y. Zhou, et al., Halide-exchanged perovskite photodetectors for wearable visible-blind ultraviolet monitoring, Nano Energy 100 (2022) 107516.
[52] W.S. Yang, et al., Iodide management in formamidinium-lead-halide-based perovskite layers for efficient solar cells, Science 356 (2017) 1376–1379.
[53] M. Saliba, et al., Cesium-containing triple cation perovskite solar cells: improved stability, reproducibility and high efficiency, Energy Environ. Sci. 9 (2016) 1989–1997.
[54] R. Riemer, A. Shapiro, Biomechanical energy harvesting from human motion: theory, state of the art, design guidelines, and future directions, J. Neuroeng. Rehabil. 8 (2011) 22.
[55] T. Starner, Human-powered wearable computing, Ibm Syst. J. 35 (1996) 618–629.
[56] Z.L. Wang, On Maxwell's displacement current for energy and sensors: the origin of nanogenerators, Mater. Today 20 (2017) 74–82.
[57] Q.Y. Li, et al., Ultra-stability high-voltage triboelectric nanogenerator designed by ternary dielectric triboelectrification with partial soft-contact and non-contact mode, Nano Energy 90 (2021) 106585.
[58] Q.Y. Li, et al., A robust constant-voltage DC triboelectric nanogenerator using the ternary dielectric triboelectrification effect, Adv. Energy Mater. 13 (2023) 2202921.
[59] X. Pu, et al., A self-charging power unit by integration of a textile triboelectric nanogenerator and a flexible lithium-ion battery for wearable electronics, Adv. Mater. 27 (2015) 2472–2478.
[60] C. Yeh, et al., Bioinspired shark skin-based liquid metal triboelectric nanogenerator for self-powered gait analysis and long-term rehabilitation monitoring, Nano Energy 104 (2022) 107852.
[61] Y. Song, et al., Wireless battery-free wearable sweat sensor powered by human motion, Sci. Adv. 6 (2020) eaay9842.
[62] Q.Y. Li, et al., Achieving ultrahigh DC-power triboelectric nanogenerators by lightning rod-inspired field emission modeling, Research 7 (2024) 0437.
[63] H.Y. Zou, et al., Quantifying and understanding the triboelectric series of inorganic non-metallic materials, Nat. Commun. 11 (2020) 2093.
[64] H.Y. Zou, et al., Quantifying the triboelectric series, Nat. Commun. 10 (2019) 1427.
[65] Q. Yi, et al., A self-powered triboelectric MXene-based 3D-printed wearable physiological biosignal sensing system for on-demand, wireless, and real-time health monitoring, Nano Energy 101 (2022) 107511.
[66] S. Jung, et al., Wearable fall detector using integrated sensors and energy devices, Sci. Rep. 5 (2015) 17081.
[67] D.J. Lu, et al., Wearable triboelectric visual sensors for tactile perception, Adv. Mater. 35 (2023) 2209117.
[68] M. Salauddin, et al., Highly electronegative V_2CT_x/Silicone nanocomposite-based serpentine triboelectric nanogenerator for wearable self-powered sensors and sign language interpretation, Adv. Energy Mater. 13 (2023) 2203812.
[69] Q. Zheng, et al., *In vivo* self-powered wireless cardiac monitoring via implantable triboelectric nanogenerator, ACS Nano 10 (2016) 6510–6518.
[70] H. Ouyang, et al., Symbiotic cardiac pacemaker, Nat. Commun. 10 (2019) 1821.
[71] R. Hinchet, et al., Transcutaneous ultrasound energy harvesting using capacitive triboelectric technology, Science 365 (2019) 491–494.
[72] Z. Liu, et al., A self-powered intracardiac pacemaker in swine model, Nat. Commun. 15 (2024) 507.
[73] Y. Zou, et al., A bionic stretchable nanogenerator for underwater sensing and energy harvesting, Nat. Commun. 10 (2019) 2695.
[74] N. Zheng, J.H. Xue, Y. Jie, X. Cao, Z.L. Wang, Wearable and humidity-resistant biomaterials-based triboelectric nanogenerator for high entropy energy harvesting and self-powered sensing, Nano Res. 15 (2022) 6213–6219.
[75] Z.H. Peng, et al., Improving relative permittivity and suppressing dielectric loss of triboelectric layers for high-performance wearable electricity generation, ACS Nano 16 (2022) 20251–20262.
[76] Z.M. Lin, et al., Triboelectric nanogenerator enabled body sensor network for self-powered human heart-rate monitoring, ACS Nano 11 (2017) 8830–8837.
[77] Y. Cao, et al., A self-powered triboelectric hybrid coder for human-machine interaction, Small Methods 6 (2022) 2101529.
[78] H.Y. Wu, et al., Ultrahigh output charge density achieved by charge trapping failure of dielectric polymers, Energy Environ. Sci. 16 (2023) 2274–2283.
[79] Q.Y. Li, et al., Overall performance improvement of direct-current triboelectric nanogenerators by charge leakage and ternary dielectric evaluation, Energy Environ. Sci. 16 (2023) 3514–3525.
[80] Q.Q. Xu, et al., Construction of flexible piezoceramic array with ultrahigh piezoelectricity via a hierarchical design strategy, Adv. Funct. Mater. 33 (2023) 2304402.
[81] S. Lee, et al., Super-flexible nanogenerator for energy harvesting from gentle wind and as an active deformation sensor, Adv. Funct. Mater. 23 (2013) 2445–2449.
[82] B.S. Athira, et al., High-performance flexible piezoelectric nanogenerator based on electrospun PVDF-$BaTiO_3$ nanofibers for self-powered vibration sensing applications, ACS Appl. Mater. Interfaces 14 (2022) 44239–44250.
[83] A. Petritz, et al., Imperceptible energy harvesting device and biomedical sensor based on ultraflexible ferroelectric transducers and organic diodes, Nat. Commun. 12 (2021) 2399.
[84] D.H. Kim, et al., In vivo self-powered wireless transmission using biocompatible flexible energy harvesters, Adv. Funct. Mater. 27 (2017) 1700341.
[85] C. Dagdeviren, et al., Conformal piezoelectric energy harvesting and storage from motions of the heart, lung, and diaphragm, PNAS 111 (2014) 1927–1932.
[86] Z.L. Wang, J.H. Song, Piezoelectric nanogenerators based on zinc oxide nanowire arrays, Science 312 (2006) 242–246.
[87] G.T. Hwang, et al., Self-powered cardiac pacemaker enabled by flexible single crystalline PMN-PT piezoelectric energy harvester, Adv. Mater. 26 (2014) 4880–4887.
[88] G.T. Hwang, et al., Self-powered deep brain stimulation *via* a flexible PIMNT energy harvester, Energy Environ. Sci. 8 (2015) 2677–2684.
[89] B. Mahanty, S.K. Ghosh, G. Prasad, A. Shanmugasundaram, D.W. Lee, Giant energy harvesting via Maxwell displacement current enhancement using metal sheet interspaced hetero-layer structured piezo-composite nanofiber device, Adv. Funct. Mater. 34 (2024) 2307723.
[90] W.L. Wang, et al., Applications of nanogenerators for biomedical engineering and healthcare systems, Infomat 4 (2022) e12262.
[91] T. Vijayakanth, et al., Perspectives on recent advancements in energy harvesting, sensing and bio-medical applications of piezoelectric gels, Chem. Soc. Rev. 52 (2023) 6191–6220.
[92] G.R. Chen, Y.Z. Li, M. Bick, J. Chen, Smart textiles for electricity generation, Chem. Rev. 120 (2020) 3668–3720.
[93] L.J. Kong, et al., A self-powered and self-sensing lower-limb system for smart healthcare, Adv. Energy Mater. 13 (2023) 2301254.
[94] M.T. Rahman, et al., Biomechanical energy-driven hybridized generator as a universal portable power source for smart/wearable electronics, Adv. Energy Mater. 10 (2020) 1903663.
[95] D.L. Wen, et al., Silk fibroin/Ag nanowire-based multifunctional sensor for wearable self-powered wireless multi-sensing microsystems, Nano Energy 113 (2023) 108569.
[96] D.J. Jiang, et al., A wearable noncontact free-rotating hybrid nanogenerator for self-powered electronics, Infomat 2 (2020) 1191–1200.
[97] Y.A. Gui, S.S. He, Y.F. Wang, J.C. Yang, MOF-derived porous Ni/C material for high-performance hybrid nanogenerator and self-powered wearable sensor, Compos. Part A-Appl. S. 168 (2023) 107492.
[98] D.L. Wen, et al., High-performance hybrid nanogenerator for self-powered wireless multi-sensing microsystems, Microsyst. Nanoeng. 9 (2023) 94.
[99] T. Quan, X. Wang, Z.L. Wang, Y. Yang, Hybridized electromagnetic-triboelectric nanogenerator for a self-powered electronic watch, ACS Nano 9 (2015) 12301–12310.
[100] S.P. Zhang, et al., Noise-less hybrid nanogenerator based on flexible WPU and siloxene composite for self-powered portable and wearable electronics, Nano Energy 120 (2024) 109179.
[101] J.Q. Zhao, et al., Remarkable merits of triboelectric nanogenerator than electromagnetic generator for harvesting small-amplitude mechanical energy, Nano Energy 61 (2019) 111–118.

[102] J. Chen, et al., A magnetic-multiplier-enabled hybrid generator with frequency division operation and high energy utilization efficiency, Research 6 (2023) 0168.
[103] M.Y. Gao, et al., Power generation for wearable systems, Energy Environ. Sci. 14 (2021) 2114–2157.
[104] J. Van Mulders, et al., Wireless power transfer: systems, circuits, standards, and use cases, Sensors 22 (2022) 5573.
[105] L. Teng, L.F. Zhu, S. Handschuh-Wang, X.C. Zhou, Robust, multiscale liquid-metal patterning enabled by a sacrificial sealing layer for flexible and wearable wireless powering, J. Mater. Chem. C. 7 (2019) 15243–15251.
[106] R. Guo, et al., Ni-GaIn amalgams enabled rapid and customizable fabrication of wearable and wireless healthcare electronics, Adv. Eng. Mater. 20 (2018) 1800054.
[107] K. Sondhi, et al., Flexible screen-printed coils for wireless power transfer using low-frequency magnetic fields, J. Micromech. Microeng. 29 (2019) 084006.
[108] A. Aldaoud, et al., Near-field wireless power transfer to stent-based biomedical implants, IEEE J. Electromagn., RF Microw. Med. Biol. 2 (2018) 193–200.
[109] J.M. Li, Y.L. Dong, J.H. Park, J. Yoo, Body-coupled power transmission and energy harvesting, Nat. Electron. 4 (2021) 530–538.
[110] R. Jegadeesan, K. Agarwal, Y.X. Guo, S.C. Yen, N.V. Thakor, Wireless power delivery to flexible subcutaneous implants using capacitive coupling, IEEE T. Microw. Theory 65 (2017) 280–292.
[111] M. El Gharbi, R. Fernández-García, S. Ahyoud, I. Gil, A review of flexible wearable antenna sensors: design, fabrication methods, and applications, Materials 13 (2020) 3781.
[112] J.S. Ho, et al., Wireless power transfer to deep-tissue microimplants, PNAS 111 (2014) 7974–7979.
[113] K.L. Montgomery, et al., Wirelessly powered, fully internal optogenetics for brain, spinal and peripheral circuits in mice, Nat. Methods 12 (2015) 969–974.
[114] D.R. Agrawal, et al., Conformal phased surfaces for wireless powering of bioelectronic microdevices, Nat. Biomed. Eng. 1 (2017) 0043.
[115] P. Gutruf, et al., Wireless, battery-free, fully implantable multimodal and multisite pacemakers for applications in small animal models, Nat. Commun. 10 (2019) 5742.
[116] Y.S. Choi, et al., Fully implantable and bioresorbable cardiac pacemakers without leads or batteries, Nat. Biotechnol. 39 (2021) 1228–1238.
[117] W.T. Dang, et al., Stretchable wireless system for sweat pH monitoring, Biosens. Bioelectron. 107 (2018) 192–202.
[118] D. Keum, et al., Wireless smart contact lens for diabetic diagnosis and therapy, Sci. Adv. 6 (2020) eaba3252.
[119] T.L. Liu, et al., Battery-free, tuning circuit-inspired wireless sensor systems for detection of multiple biomarkers in bodily fluids, Sci. Adv. 8 (2022) eabo7049.
[120] W.S. Kim, et al., Organ-specific, multimodal, wireless optoelectronics for high-throughput phenotyping of peripheral neural pathways, Nat. Commun. 12 (2021) 157.
[121] X. Zhang, et al., Two-dimensional MoS_2-enabled flexible rectenna for Wi-Fi-band wireless energy harvesting, Nature 566 (2019) 368–372, https://doi.org/10.1038/s41586-019-0892-1.
[122] A. Singer, et al., Magnetoelectric materials for miniature, wireless neural stimulation at therapeutic frequencies, Neuron 107 (2020) 631–643.
[123] J.C. Chen, et al., A wireless millimetric magnetoelectric implant for the endovascular stimulation of peripheral nerves, Nat. Biomed. Eng. 6 (2022) 706–716.
[124] Z.H. Yu, et al., MagNI: a magnetoelectrically powered and controlled wireless neurostimulating implant, IEEE Trans. Biomed. Circuits Syst. 14 (2020) 1241–1252.
[125] Z.H. Yu, et al., Magnetoelectric bio-implants powered and programmed by a single transmitter for coordinated multisite stimulation, IEEE J. Solid-St. Circ. 57 (2022) 818–830.
[126] M. Thielen, L. Sigrist, M. Magno, C. Hierold, L. Benini, Human body heat for powering wearable devices: from thermal energy to application, Energ. Convers. Manag. 131 (2017) 44–54.
[127] S.Z. Lyu, et al., Subcutaneous power supply by NIR-II light, Nat. Commun. 13 (2022) 6596.
[128] F.T. Alrashdan, et al., Wearable wireless power systems for 'ME-BIT' magnetoelectric-powered bio implants, J. Neural Eng. 18 (2021) 045011.
[129] A.T. Yahiro, S.M. Lee, D.O. Kimble, Bioelectrochemistry: I. Enzyme utilizing bio-fuel cell studies, Biochim. Biophys. Acta 88 (1964) 375–383.
[130] J. Moyer, D. Wilson, I. Finkelshtein, B. Wong, R. Potts, Correlation between sweat glucose and blood glucose in subjects with diabetes, Diabetes Technol. The. 14 (2012) 398–402.
[131] X.F. Jin, A. Cai, T.L. Xu, X.J. Zhang, Artificial intelligence biosensors for continuous glucose monitoring, Interdiscip. Mater. 2 (2023) 290–307.
[132] S. Gupta, S.V. Sandhu, H. Bansal, D. Sharma, Comparison of salivary and serum glucose levels in diabetic patients, J. Diabetes Sci. Technol. 9 (2014) 91–96.
[133] J.M. Green, R.C. Pritchett, T.R. Crews, J.R. McLester, D.C. Tucker, Sweat lactate response between males with high and low aerobic fitness, Eur. J. Appl. Physiol. 91 (2004) 1–6.
[134] R.C. Reid, S.D. Minteer, B.K. Gale, Contact lens biofuel cell tested in a synthetic tear solution, Biosens. Bioelectron. 68 (2015) 142–148.
[135] H. Lee, et al., A graphene-based electrochemical device with thermoresponsive microneedles for diabetes monitoring and therapy, Nat. Nanotech 11 (2016) 566–572.
[136] P.O. Conghaile, et al., Fully enzymatic membraneless glucose/oxygen fuel cell that provides 0.275 mA cm^{-2} in 5 mM glucose, operates in human physiological solutions, and powers transmission of sensing data, Anal. Chem. 88 (2016) 2156–2163.
[137] X.X. Xiao, et al., Tackling the challenges of enzymatic (bio)fuel cells, Chem. Rev. 119 (2019) 9509–9558.
[138] W.Z. Jia, G. Valdés-Ramírez, A.J. Bandodkar, J.R. Windmiller, J. Wang, Epidermal biofuel cells: energy harvesting from human perspiration, Angew. Chem. Int. Ed. 52 (2013) 7233–7236.
[139] J.H. Min, et al., Skin-interfaced wearable sweat sensors for precision medicine, Chem. Rev. 123 (2023) 5049–5138.
[140] J.S. del Rio, O.Y.F. Henry, P. Jolly, D.E. Ingber, An antifouling coating that enables affinity-based electrochemical biosensing in complex biological fluids, Nat. Nanotechnol. 14 (2019) 1143–1149.
[141] M. Bariya, H.Y.Y. Nyein, A. Javey, Wearable sweat sensors, Nat. Electron. 1 (2018) 160–171.
[142] G. Güven, R. Prodanovic, U. Schwaneberg, Protein engineering - an option for enzymatic biofuel cell design, Electroanalysis 22 (2010) 765–775.
[143] S. Krishnan, F.A. Armstrong, Order-of-magnitude enhancement of an enzymatic hydrogen-air fuel cell based on pyrenyl carbon nanostructures, Chem. Sci. 3 (2012) 1015–1023.
[144] D. Wen, A. Eychmüller, Enzymatic biofuel cells on porous nanostructures, Small 12 (2016) 4649–4661.
[145] C.H. Kwon, et al., High-power hybrid biofuel cells using layer-by-layer assembled glucose oxidase-coated metallic cotton fibers, Nat. Commun. 9 (2018) 4479.
[146] L.N. Zhong, et al., Stretchable liquid metal-based metal-polymer conductors for fully screen-printed biofuel cells, Anal. Chem. 94 (2022) 16738–16745.
[147] G. Valdés-Ramírez, et al., Microneedle-based self-powered glucose sensor, Electrochem. Commun. 47 (2014) 58–62.
[148] I. Jeerapan, W. Sangsudcha, P. Phokhonwong, Wearable energy devices on mask-based printed electrodes for self-powered glucose biosensors, Sens. Bio-Sens. Res. 38 (2022) 100525.
[149] S.J. Yin, Z.W. Jin, T. Miyake, Wearable high-powered biofuel cells using enzyme/carbon nanotube composite fibers on textile cloth, Biosens. Bioelectron. 141 (2019) 111471.
[150] K. Veenuttranon, K. Kaewpradub, I. Jeerapan, Screen-printable functional nanomaterials for flexible and wearable single-enzyme-based energy-harvesting and self-powered biosensing devices, Nano-Micro Lett. 15 (2023) 85.
[151] C.H. Kwon, et al., High-power biofuel cell textiles from woven biscrolled carbon nanotube yarns, Nat. Commun. 5 (2014) 3928.
[152] R.A. Escalona-Villalpando, et al., Clean energy from human sweat using an enzymatic patch, J. Power Sources 412 (2019) 496–504.
[153] J. Lv, et al., Sweat-based wearable energy harvesting-storage hybrid textile devices, Energy Environ. Sci. 11 (2018) 3431–3442.
[154] X.H. Chen, et al., Stretchable and flexible buckypaper-based lactate biofuel cell for wearable electronics, Adv. Funct. Mater. 29 (2019) 1905785.
[155] A.J. Bandodkar, et al., Soft, stretchable, high power density electronic skin-based biofuel cells for scavenging energy from human sweat, Energy Environ. Sci. 10 (2017) 1581–1589.
[156] Y. Yu, et al., Biofuel-powered soft electronic skin with multiplexed and wireless sensing for human-machine interfaces, Sci. Robot. 5 (2020) eaaz7946.
[157] I. Shitanda, et al., Self-powered diaper sensor with wireless transmitter powered by paper-based biofuel cell with urine glucose as fuel, ACS Sens 6 (2021) 3409–3415.
[158] J.R. Zhang, et al., A wearable self-powered biosensor system integrated with diaper for detecting the urine glucose of diabetic patients, Sens. Actuat. B-Chem. 341 (2021) 130046.
[159] Y. Ogawa, et al., Organic transdermal iontophoresis patch with built-in biofuel cell, Adv. Healthc. Mater. 4 (2015) 506–510.
[160] S.I. Kim, et al., Dense dislocation arrays embedded in grain boundaries for high-performance bulk thermoelectrics, Science 348 (2015) 109–114.
[161] L. Li, W.D. Liu, Q.F. Liu, Z.G. Chen, Multifunctional wearable thermoelectrics for personal thermal management, Adv. Funct. Mater. 32 (2022) 2200548.
[162] X.L. Shi, J. Zou, Z.G. Chen, Advanced thermoelectric design: from materials and structures to devices, Chem. Rev. 120 (2020) 7399–7515.
[163] Q.H. Zhang, K.F. Deng, L. Wilkens, H. Reith, K. Nielsch, Micro-thermoelectric devices, Nat. Electron. 5 (2022) 333–347.
[164] M. Mukaida, K. Kirihara, S. Horike, Q.S. Wei, Stable organic thermoelectric devices for self-powered sensor applications, J. Mater. Chem. A 8 (2020) 22544–22556.
[165] Z.J. An, et al., Body heat powered wirelessly wearable system for real-time physiological and biochemical monitoring, Adv. Funct. Mater. 33 (2023) 2303361.
[166] S.J. Zhu, et al., Persistently self-powered wearable thermoelectric generator enabled by phase-change inorganics as the heat sink, Mater. Today Phys. 32 (2023) 101011.
[167] J.F. Yuan, Y.Z. Zhang, C.S. Wei, R. Zhu, A fully self-powered wearable leg movement sensing system for human health monitoring, Adv. Sci. 10 (2023) 2303114.
[168] Y. Wang, Y.G. Shi, D.Q. Mei, Z.C. Chen, Wearable thermoelectric generator to harvest body heat for powering a miniaturized accelerometer, Appl. Energy 215 (2018) 690–698.
[169] A. Tanwar, S. Lal, K.M. Razeeb, Structural design optimization of micro-thermoelectric generator for wearable biomedical devices, Energies 14 (2021) 2339.
[170] C.G. Han, et al., Giant thermopower of ionic gelatin near room temperature, Science 368 (2020) 1091–1098.
[171] S. Yang, et al., Flexible thermoelectric generator and energy management electronics powered by body heat, Microsyst. Nanoeng. 9 (2023) 106.

[172] M. Hyland, H. Hunter, J. Liu, E. Veety, D. Vashaee, Wearable thermoelectric generators for human body heat harvesting, Appl. Energy 182 (2016) 518–524.
[173] B. Lee, et al., High-performance compliant thermoelectric generators with magnetically self-assembled soft heat conductors for self-powered wearable electronics, Nat. Commun. 11 (2020) 5948.
[174] X.L. Ma, J. Zhao, D.H. Shou, Y. Liu, A highly-flexible and breathable photo-thermo-electric membrane for energy harvesting, Adv. Energy Mater. 14 (2024) 2304032.
[175] S.J. Kim, J.H. We, B.J. Cho, A wearable thermoelectric generator fabricated on a glass fabric, Energy Environ. Sci. 7 (2014) 1959–1965.
[176] W. Liu, et al., A liquid metal-enhanced wearable thermoelectric generator, Bioeng. -Basel 9 (2022) 254.
[177] H. You, et al., Flexible Bi_2Te_3-based thermoelectric generator with an ultra-high power density, Appl. Therm. Eng. 202 (2022) 117818.
[178] Y.L. Wang, et al., High-performance stretchable organic thermoelectric generator via rational thermal interface design for wearable electronics, Adv. Energy Mater. 12 (2022) 2102835.
[179] M.H. Malakooti, et al., Liquid metal supercooling for low-temperature thermoelectric wearables, Adv. Funct. Mater. 29 (2019) 1906098.
[180] F. Deng, H.B. Qiu, J. Chen, L. Wang, B. Wang, Wearable thermoelectric power generators combined with flexible supercapacitor for low-power human diagnosis devices, IEEE Trans. Ind. Electron. 64 (2017) 1477–1485.
[181] J.R. Lv, J.L. Ma, L. Dai, T. Yin, Z.Z. He, A high-performance wearable thermoelectric generator with comprehensive optimization of thermal resistance and voltage boosting conversion, Appl. Energy 312 (2022) 118696.
[182] G.Y. Hu, H. Edwards, M. Lee, Silicon integrated circuit thermoelectric generators with a high specific power generation capacity, Nat. Electron. 2 (2019) 300–306.
[183] Z.H. Zhang, et al., Emerging hydrovoltaic technology, Nat. Nanotech 13 (2018) 1109–1119.
[184] F. Zhao, H.H. Cheng, Z.P. Zhang, L. Jiang, L.T. Qu, Direct power generation from a graphene oxide film under moisture, Adv. Mater. 27 (2015) 4351–4357.
[185] X.M. Liu, et al., Power generation from ambient humidity using protein nanowires, Nature 578 (2020) 550–554.
[186] T. Xu, X.T. Ding, H.H. Cheng, G.Y. Han, L.T. Qu, Moisture-enabled electricity from hygroscopic materials: a new type of clean energy, Adv. Mater. 36 (2024) 2209661.
[187] Q.M. Wei, et al., Moisture electricity generation: Mechanisms, structures, and applications, Nano Res. 16 (2023) 7496–7510.
[188] Y. Zhang, et al., Sustainable power generation for at least one month from ambient humidity using unique nanofluidic diode, Nat. Commun. 13 (2022) 3484.
[189] T.C. He, et al., Fully printed planar moisture-enabled electric generator arrays for scalable function integration, Joule 7 (2023) 935–951.
[190] B.B. Shao, et al., Bioinspired hierarchical nanofabric electrode for silicon hydrovoltaic device with record power output, ACS Nano 15 (2021) 7472–7481.
[191] Y. Liang, et al., Electric power generation via asymmetric moisturizing of graphene oxide for flexible, printable and portable electronics, Energy Environ. Sci. 11 (2018) 1730–1735.
[192] N. Chen, et al., MEG actualized by high-valent metal carrier transport, Nano Energy 65 (2019) 104047.
[193] S. Yang, et al., Green moisture-electric generator based on supramolecular hydrogel with tens of milliamp electricity toward practical applications, Nat. Commun. 15 (2024) 3329.
[194] F. Zhao, Y. Liang, H.H. Cheng, L. Jiang, L.T. Qu, Highly efficient moisture-enabled electricity generation from graphene oxide frameworks, Energy Environ. Sci. 9 (2016) 912–916.
[195] Y.X. Huang, et al., Interface-mediated hygroelectric generator with an output voltage approaching 1.5 volts, Nat. Commun. 9 (2018) 4166.
[196] K. Han, D.D. Zhang, W.B. Zhuang, Y.F. Wan, P. Yang, Integrated multimodal microfluidic E-skin powered by synergistic tandem nanogenerators for sweat-based health monitoring and skin-temperature analysis, J. Mater. Chem. A 11 (2023) 17112–17124.
[197] Q.J. Li, et al., Moist-electric generator with efficient output and scalable integration based on carbonized polymer dot and liquid metal active electrode, Adv. Funct. Mater. 33 (2023) 2211013.
[198] H.H. Cheng, et al., Spontaneous power source in ambient air of a well-directionally reduced graphene oxide bulk, Energy Environ. Sci. 11 (2018) 2839–2845.
[199] Y.X. Huang, H.H. Cheng, L.T. Qu, Emerging materials for water-enabled electricity generation, ACS Mater. Lett. 3 (2021) 193–209.
[200] R.B. Zhu, et al., Lab free protein-based moisture electric generators with a high electric output, Energy Environ. Sci. 16 (2023) 2338–2345.
[201] X.W. Nie, et al., Gradient doped polymer nanowire for moistelectric nanogenerator, Nano Energy 46 (2018) 297–304.
[202] Z.H. Kou, et al., Wearable all-fabric hybrid energy harvester to simultaneously harvest radiofrequency and triboelectric energy, Adv. Sci. 11 (2024) 2309050.
[203] J. Chen, et al., Micro-cable structured textile for simultaneously harvesting solar and mechanical energy, Nat. Energy 1 (2016) 16138.
[204] Z. Wen, et al., Self-powered textile for wearable electronics by hybridizing fiber-shaped nanogenerators, solar cells, and supercapacitors, Sci. Adv. 2 (2016) e1600097.
[205] W. Yan, et al., Self-powered and wireless physiological monitoring system with integrated power supply and sensors, Nano Energy 108 (2023) 108203.
[206] P.C. Tan, et al., A battery-like self-charge universal module for motional energy harvest, Adv. Energy Mater. 9 (2019) 1901875.
[207] L. Yin, et al., A self-sustainable wearable multi-modular E-textile bioenergy microgrid system, Nat. Commun. 12 (2021) 1542.
[208] G. Kim, et al., A deformable complementary moisture and tribo energy harvester, Energy Environ. Sci. 17 (2024) 134–148.
[209] L. Yin, et al., A passive perspiration biofuel cell: High energy return on investment, Joule 5 (2021) 1888–1904.
[210] L. Xu, et al., Giant voltage enhancement *via* triboelectric charge supplement channel for self-powered electroadhesion, ACS Nano 12 (2018) 10262–10271.
[211] A. Ghaffarinejad, J.Y. Hasani, D. Galayko, P. Basset, Superior performance of half-wave to full-wave rectifier as a power conditioning circuit for triboelectric nanogenerators: Application to contact-separation and sliding mode TENG, Nano Energy 66 (2019) 104137.
[212] Z. Wang, et al., Two voltages in contact-separation triboelectric nanogenerator: From asymmetry to symmetry for maximum output, Nano Energy 69 (2020) 104452.
[213] G. Zhu, J. Chen, T.J. Zhang, Q.S. Jing, Z.L. Wang, Radial-arrayed rotary electrification for high performance triboelectric generator, Nat. Commun. 5 (2014) 3426.
[214] W.L. Liu, et al., Integrated charge excitation triboelectric nanogenerator, Nat. Commun. 10 (2019) 1426.
[215] W.L. Liu, Z. Wang, C.G. Hu, Advanced designs for output improvement of triboelectric nanogenerator system, Mater. Today 45 (2021) 93–119.
[216] M. Miyatake, M. Veerachary, F. Toriumi, N. Fujii, H. Ko, Maximum power point tracking of multiple photovoltaic arrays: A PSO approach, IEEE T. Aero. Elec. Sys. 47 (2011) 367–380.
[217] A. Zebda, et al., Single glucose biofuel cells implanted in rats power electronic devices, Sci. Rep. 3 (2013) 1516.
[218] T. Esram, P.L. Chapman, Comparison of photovoltaic array maximum power point tracking techniques, IEEE T. Energy Conver. 22 (2007) 439–449.
[219] G.K. Ottman, H.F. Hofmann, A.C. Bhatt, G.A. Lesieutre, Adaptive piezoelectric energy harvesting circuit for wireless remote power supply, IEEE Trans. Power Electron. 17 (2002) 669–676.
[220] S. Lineykin, S. Ben-Yaakov, Modeling and analysis of thermoelectric modules, IEEE T. Ind. Appl. 43 (2007) 505–512.
[221] M. Dini, et al., A nanocurrent power management IC for multiple heterogeneous energy harvesting sources, IEEE Trans. Power Electron. 30 (2015) 5665–5680.
[222] Z. Wang, et al., Giant performance improvement of triboelectric nanogenerator systems achieved by matched inductor design, Energy Environ. Sci. 14 (2021) 6627–6637.
[223] Z. Wang, et al., Ultrahigh electricity generation from low-frequency mechanical energy by efficient energy management, Joule 5 (2021) 441–455.
[224] W.L. Liu, et al., Switched-capacitor-convertors based on fractal design for output power management of triboelectric nanogenerator, Nat. Commun. 11 (2020) 1883.
[225] T. Hanashi, et al., BioCapacitor-A novel category of biosensor, Biosens. Bioelectron. 24 (2009) 1837–1842.
[226] W. Tang, et al., A power-transformed-and-managed triboelectric nanogenerator and its applications in a self-powered wireless sensing node, Nanotechnology 25 (2014) 225402.
[227] F.B. Xi, et al., Universal power management strategy for triboelectric nanogenerator, Nano Energy 37 (2017) 168–176.
[228] W. Harmon, D. Bamgboje, H.Y. Guo, T.S. Hu, Z.L. Wang, Self-driven power management system for triboelectric nanogenerators, Nano Energy 71 (2020) 104642.
[229] H.F. Qin, et al., High energy storage efficiency triboelectric nanogenerators with unidirectional switches and passive power management circuits, Adv. Funct. Mater. 28 (2018) 1805216.
[230] L.C. Luo, D.C. Bao, W.Q. Yu, Z.H. Zhang, T.L. Ren, A low input current and wide conversion ratio buck regulator with 75% efficiency for high-voltage triboelectric nanogenerators, Sci. Rep. 6 (2016) 19246.
[231] S.M. Niu, X.F. Wang, F. Yi, Y.S. Zhou, Z.L. Wang, A universal self-charging system driven by random biomechanical energy for sustainable operation of mobile electronics, Nat. Commun. 6 (2015) 8975.
[232] J.J. Yang, et al., Managing and optimizing the output performances of a triboelectric nanogenerator by a self-powered electrostatic vibrator switch, Nano Energy 46 (2018) 220–228.
[233] Y. Song, et al., High-efficiency self-charging smart bracelet for portable electronics, Nano Energy 55 (2019) 29–36.
[234] H.M. Zhang, et al., Employing a MEMS plasma switch for conditioning high-voltage kinetic energy harvesters, Nat. Commun. 11 (2020) 3221.
[235] G. Cheng, et al., Managing and maximizing the output power of a triboelectric nanogenerator by controlled tip-electrode air-discharging and application for UV sensing, Nano Energy 44 (2018) 208–216.
[236] Y. Jang, S.M. Kim, G.M. Spinks, S.J. Kim, Carbon nanotube yarn for fiber-shaped electrical sensors, actuators, and energy storage for smart systems, Adv. Mater. 32 (2020) 2070034.
[237] P.Y. Ji, et al., Achieving continuous self-powered energy conversion-storage-supply integrated system based on carbon felt, Adv. Sci. 10 (2023) 2207033.
[238] A. Yona, et al., Application of neural network to 24-hour-ahead generating power forecasting for PV system, IEEE Power Energy Soc. Gen. Meet. - Convers. Deliv. Electr. Energy 21st Century 2008 (2008) 1–6.
[239] P.V. Mahesh, S. Meyyappan, R. Alla, Maximum power point tracking with regression machine learning algorithms for solar PV systems, Int. J. Renew. Energy Res. 12 (2022) 1327–1338.
[240] J. Heikenfeld, et al., Wearable sensors: modalities, challenges, and prospects, Lab a Chip 18 (2018) 217–248.

[241] W. Gao, et al., Fully integrated wearable sensor arrays for multiplexed *in situ* perspiration analysis, Nature 529 (2016) 509–514.
[242] C. Zhao, J. Park, S.E. Root, Z. Bao, Skin-inspired soft bioelectronic materials, devices and systems, Nat. Rev. Bioeng. (2024), https://doi.org/10.1038/s44222-024-00194-1.
[243] S.Q. Guo, et al., Integrated contact lens sensor system based on multifunctional ultrathin MoS_2 transistors, Matter 4 (2021) 969–985.
[244] J. Kim, A.S. Campbell, B.E.F. de Avila, J. Wang, Wearable biosensors for healthcare monitoring, Nat. Biotechnol. 37 (2019) 389–406.
[245] H.A. Yigit, et al., A pulse-width modulated cochlear implant interface electronics with 513 μW power consumption, IEEE/ACM Int. Symp. . Low. Power Electron. Des. (ISLPED) (2019) 1–5, https://doi.org/10.1109/ISLPED.2019.8824838.
[246] J. Dieffenderfer, et al., Low-power wearable systems for continuous monitoring of environment and health for chronic respiratory disease, IEEE J. Biomed. Health Inform. 20 (2016) 1251–1264.
[247] C.X. Zhu, et al., Stretchable temperature-sensing circuits with strain suppression based on carbon nanotube transistors, Nat. Electron. 1 (2018) 183–190.
[248] C.C. Huang, Z.K. Kao, Y.C. Liao, Flexible miniaturized nickel oxide thermistor arrays via inkjet printing technology, ACS Appl. Mater. Interfaces 5 (2013) 12954–12959.
[249] S. Kano, K. Kim, M. Fujii, Fast-response and flexible nanocrystal-based humidity sensor for monitoring human respiration and water evaporation on skin, ACS Sens 2 (2017) 828–833.
[250] C.Y. Yan, J.X. Wang, P.S. Lee, Stretchable graphene thermistor with tunable thermal index, ACS Nano 9 (2015) 2130–2137.
[251] S. Gong, et al., A wearable and highly sensitive pressure sensor with ultrathin gold nanowires, Nat. Commun. 5 (2014) 3132.
[252] G. Schwartz, et al., Flexible polymer transistors with high pressure sensitivity for application in electronic skin and health monitoring, Nat. Commun. 4 (2013) 1859.
[253] H. Zhang, et al., Wireless, battery-free optoelectronic systems as subdermal implants for local tissue oximetry, Sci. Adv. 5 (2019) eaaw0873.
[254] J. Kim, et al., Self-charging wearables for continuous health monitoring, Nano Energy 79 (2021) 105419.
[255] Y.D. Yu, et al., Wearable respiration sensor for continuous healthcare monitoring using a micro-thermoelectric generator with rapid response time and chip-level design, Adv. Mater. Technol. 7 (2022) 2101416.
[256] L.L. Zu, et al., Multiangle, self-powered sensor array for monitoring head impacts, Sci. Adv. 9 (2023) eadg5152.
[257] L. Su, Q. Xiong, H.Y. Wang, Y.L. Zi, Porous-structure-promoted tribo-induced high-performance self-powered tactile sensor toward remote human-machine interaction, Adv. Sci. 9 (2022) 2203510.
[258] C.Y. Li, et al., Sensing of joint and spinal bending or stretching via a retractable and wearable badge reel, Nat. Commun. 12 (2021) 2950.
[259] C.Y. Tang, et al., Unconstrained piezoelectric vascular electronics for wireless monitoring of hemodynamics and cardiovascular health, Small 20 (2024) 2304752.
[260] D.Y. Park, et al., Self-powered real-time arterial pulse monitoring using ultrathin epidermal piezoelectric sensors, Adv. Mater. 29 (2017) 1702308.
[261] K.Y. Meng, et al., A wireless textile-based sensor system for self-powered personalized health care, Matter 2 (2020) 896–907.
[262] H.Y. Guo, et al., A highly sensitive, self-powered triboelectric auditory sensor for social robotics and hearing aids, Sci. Robot. 3 (2018) eaat2516.
[263] X. Peng, et al., A breathable, biodegradable, antibacterial, and self-powered electronic skin based on all-nanofiber triboelectric nanogenerators, Sci. Adv. 6 (2020) eaba9624.
[264] B.B. Shao, et al., Large-area, untethered, metamorphic, and omnidirectionally stretchable multiplexing self-powered triboelectric skins, Nat. Commun. 15 (2024) 1238.
[265] K. Tao, et al., Deep-learning enabled active biomimetic multifunctional hydrogel electronic skin, ACS Nano 17 (2023) 16160–16173.
[266] M. Kang, et al., Self-powered temperature electronic skin based on island-bridge structure and Bi-Te micro-thermoelectric generator for distributed mini-region sensing, Adv. Mater. 35 (2023) 2309629.
[267] H.L. Yu, et al., Flexible temperature-pressure dual sensor based on 3D spiral thermoelectric Bi_2Te_3 films, Nat. Commun. 15 (2024) 2521.
[268] L.H. Li, et al., Moisture-driven power generation for multifunctional flexible sensing systems, Nano Lett. 19 (2019) 5544–5552.
[269] K. Tao, et al., Ultra-sensitive, deformable, and transparent triboelectric tactile sensor based on micro-pyramid patterned ionic hydrogel for interactive human-machine interfaces, Adv. Sci. 9 (2022) 2104168.
[270] B. Zhou, et al., Matrix-addressed crosstalk-free self-powered pressure sensor array based on electrospun isolated PVDF-TrFE cells, Sens. Actuator A Phys. 347 (2022) 113993.
[271] J.C. Li, J. Yin, M.G.V. Wee, A. Chinnappan, S. Ramakrishna, A self-powered piezoelectric nanofibrous membrane as wearable tactile sensor for human body motion monitoring and recognition, Adv. Fiber Mater. 5 (2023) 1417–1430.
[272] C.Y. Du, et al., Toward precision recognition of complex hand motions: wearable thermoelectrics by synergistic 2D nanostructure confinement and controlled reduction, Adv. Funct. Mater. 32 (2022) 2206083.
[273] P.C. Tan, et al., Self-powered gesture recognition wristband enabled by machine learning for full keyboard and multicommand input, Adv. Mater. 34 (2022) 2200793.
[274] M.L. Zhu, et al., Haptic-feedback smart glove as a creative human-machine interface (HMI) for virtual/augmented reality applications, Sci. Adv. 6 (2020) eaaz8693.
[275] Z.H. Guo, et al., A wearable multidimensional motion sensor for AI-enhanced VR sports, Research 6 (2023) 0154.
[276] Y. Song, D. Mukasa, H.X. Zhang, W. Gao, Self-powered wearable biosensors, Acc. Mater. Res. 2 (2021) 184–197.
[277] C.W. Bae, M.V. Chinnamani, E.H. Lee, N.E. Lee, Stretchable non-enzymatic fuel cell-based sensor patch integrated with thread-embedded microfluidics for self-powered wearable glucose monitoring, Adv. Mater. Interfaces 9 (2022) 2200492.
[278] A.J. Bandodkar, et al., Battery-free, skin-interfaced microfluidic/electronic systems for simultaneous electrochemical, colorimetric, and volumetric analysis of sweat, Sci. Adv. 5 (2019) eaav3294.
[279] X.C. Huang, et al., Epidermal self-powered sweat sensors for glucose and lactate monitoring, Bio-Des. Manuf. 5 (2022) 201–209.
[280] D.P. Rose, et al., Adhesive RFID sensor patch for monitoring of sweat electrolytes, IEEE T. Biomed. Eng. 62 (2015) 1457–1465.
[281] Y. Dong, et al., A "two-part" resonance circuit based detachable sweat patch for noninvasive biochemical and biophysical sensing, Adv. Funct. Mater. 33 (2023) 2210136.
[282] S. Li, et al., Bioresorbable, wireless, passive sensors for continuous pH measurements and early detection of gastric leakage, Sci. Adv. 10 (2024) eadj0268.
[283] Z.K. Li, et al., Power-free contact lens for glucose sensing, Adv. Funct. Mater. 33 (2023) 2304647.
[284] X. Li, et al., All-MXene-printed RF resonators as wireless plant wearable sensors for in situ ethylene detection, Small 19 (2023) 2207889.
[285] X.L. Tong, et al., Multifunctional fiber for synchronous bio-sensing and power supply in sweat environment, Adv. Funct. Mater. 33 (2023) 2301174.
[286] K. Dong, X. Peng, Z.L. Wang, Fiber/fabric-based piezoelectric and triboelectric nanogenerators for flexible/stretchable and wearable electronics and artificial intelligence, Adv. Mater. 32 (2020) 1902549.
[287] J.F. Wu, S.S. He, J.Q. Li, A.G. Song, Cable crosstalk suppression with two-wire voltage feedback method for resistive sensor array, Sensors 16 (2016) 253.
[288] G.M. Whitesides, The origins and the future of microfluidics, Nature 442 (2006) 368–373.
[289] M. Safarkhani, et al., Integration of MXene and microfluidics: a perspective, Acs Biomater. S. Sci. Eng. 10 (2024) 657–676.
[290] A.A. Yazdi, et al., 3D printing: an emerging tool for novel microfluidics and lab-on-a-chip applications, Microfluid. Nanofluidics 20 (2016) 50.
[291] X.K. Kong, P.P. Gai, L. Ge, F. Li, Laser-scribed *N*-doped graphene for integrated flexible enzymatic biofuel cells, ACS Sustain. Chem. Eng. 8 (2020) 12437–12442.
[292] S. Shin, et al., High-performance screen-printed thermoelectric films on fabrics, Sci. Rep. 7 (2017) 7317.
[293] D. Shukla, Y.X. Liu, Y. Zhu, Eco-friendly screen printing of silver nanowires for flexible and stretchable electronics, Nanoscale 15 (2023) 2767–2778.
[294] J.R. Sempionatto, et al., Eyeglasses based wireless electrolyte and metabolite sensor platform, Lab a Chip 17 (2017) 1834–1842.
[295] R.S. Chen, M.Y. Gao, D.W. Chu, W.L. Cheng, Y.R. Lu, Self-powered hydrogel wearable bioelectronics, Nano Energy 128 (2024) 109960.
[296] C.H. Wang, et al., Monitoring of the central blood pressure waveform via a conformal ultrasonic device, Nat. Biomed. Eng. 2 (2018) 687–695.
[297] K. Kim, B. Kim, C.H. Lee, Printing flexible and hybrid electronics for human skin and eye-interfaced health monitoring systems, Adv. Mater. 32 (2020) 1902051.
[298] C.F. Wang, C.H. Wang, Z.L. Huang, S. Xu, Materials and structures toward soft electronics, Adv. Mater. 30 (2018) 1801368.
[299] Q. Zhuang, et al., Permeable, three-dimensional integrated electronic skins with stretchable hybrid liquid metal solders, Nat. Electron. 7 (2024) 598–609.
[300] K. Myny, The development of flexible integrated circuits based on thin-film transistors, Nat. Electron. 1 (2018) 30–39.
[301] Z.L. Li, W.W. Li, Y.T. Liu, M. Xun, M.C. Yuan, Study of heat transfer performance of miniature heat sink for integrated circuit packaging field, Case Stud. Therm. Eng. 49 (2023) 103290.
[302] S. Xu, et al., Soft microfluidic assemblies of sensors, circuits, and radios for the skin, Science 344 (2014) 70–74.
[303] X.H. Zhang, et al., A low-power wide-area network information monitoring system by combining NB-IoT and LoRa, IEEE Internet Things J. 6 (2019) 590–598.
[304] F. Moreno-Cruz, et al., *treNch*: Ultra-low power wireless communication protocol for IoT and energy harvesting, Sensors 20 (2020) 6156.
[305] K. Kwon, et al., A battery-less wireless implant for the continuous monitoring of vascular pressure, flow rate and temperature, Nat. Biomed. Eng. 7 (2023) 1215–1228.
[306] B. Kellogg, V. Talla, J.R. Smith, S. Gollakot, PASSIVE WI-FI: bringing low power to Wi-Fi transmissions, GetMobile: Mob. Comp. Comm. 20 (2017) 38–41.
[307] B. Kellogg, V. Talla, S. Gollakota, J.R. Smith, U. Assoc, Passive Wi-Fi: Bringing Low Power to Wi-Fi Transmissions, 13th USENIX Symp. . Netw. Syst. Des. Implement. (NSDI) (2016) 151–164.
[308] J.D. MacKenzie, C. Ho, Perspectives on energy storage for flexible electronic systems, Proc. Ieee 103 (2015) 535–553.
[309] J. Park, et al., Soft, smart contact lenses with integrations of wireless circuits, glucose sensors, and displays, Sci. Adv. 4 (2018) eaap9841.
[310] Z.H. Shi, et al., Wearable battery-free theranostic dental patch for wireless intraoral sensing and drug delivery, npj Flex. Electron. 6 (2022) 49.
[311] M.R. Sohail, et al., Risk factor analysis of permanent pacemaker infection, Clin. Infect. Dis. 45 (2007) 166–173.
[312] F.V.Y. Tjong, V.Y. Reddy, Permanent leadless cardiac pacemaker therapy: a comprehensive review, Circulation 135 (2017) 1458–1470.
[313] J.C. Lin, A new IEEE standard for safety levels with respect to human exposure to radio-frequency radiation, IEEE Antennas Propag. Mag. 48 (2006) 157–159.

[314] S.M. Niu, et al., A wireless body area sensor network based on stretchable passive tags, Nat. Electron. 2 (2019) 361–368.
[315] H.W. Choi, et al., Smart textile lighting/display system with multifunctional fibre devices for large scale smart home and IoT applications, Nat. Commun. 13 (2022) 814.
[316] W.F. Yang, et al., Single body-coupled fiber enables chipless textile electronics, Science 384 (2024) 74–81.
[317] J. Si, et al., A carbon-nanotube-based tensor processing unit, Nat. Electron. 7 (2024) 684–693.
[318] S.Y. Wang, X.X. Liu, P. Zhou, The road for 2D semiconductors in the silicon age, Adv. Mater. 34 (2022) 2106886.
[319] S.P. Senanayak, et al., Understanding charge transport in lead iodide perovskite thin-film field-effect transistors, Sci. Adv. 3 (2017) e1601935.
[320] K.R.G. Lim, et al., Fundamentals of MXene synthesis, Nat. Synth. 1 (2022) 601–614.
[321] J. Pei, et al., Towards artificial general intelligence with hybrid Tianjic chip architecture, Nature 572 (2019) 106–111.
[322] H.W. Tan, Y.F. Zhou, Q.Z. Tao, J. Rosen, S. van Dijken, Bioinspired multisensory neural network with crossmodal integration and recognition, Nat. Commun. 12 (2021) 1120.

Qianying Li received her B.S. degree in Physics from Chongqing Technology and Business University in 2018. She is a PhD student in the field of Physics, Chongqing University. Now, she is a visiting PhD student at Australian National University. Currently, her research interests are mainly focused on improving the output performance of triboelectric nanogenerator and triboelectric nanogenerator based on two-dimensional materials.

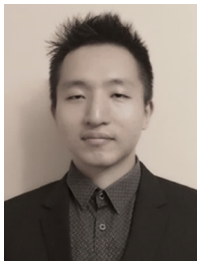

Mingyuan Gao is a Senior Editor of the IEEE Transactions on Intelligent Transportation Systems, an Associate Professor at the College of Engineering and Technology at Southwest University, China, and a Postdoctoral Researcher at the College of Engineering and Computer Science at the Australian National University. He earned his BE and ME degrees from Huazhong University of Science and Technology, China, in 2008 and 2010, respectively, and his PhD degree from Southwest Jiaotong University in 2018. He was a Senior Engineer at Siemens AG from 2011 to 2018. His research interests include flexible electronics, energy harvesting, self-powered monitoring, and nonlinear dynamics. He won the 2010 GE Foundation TECH Award-First Place Award.

Xueqian Sun received her B.E. and Ph.D. degrees from the Australian National University in the School of Engineering in 2017 and 2024, respectively. She is currently working as a Research Fellow at ANU. Her research interests include the nano-engineering of exciton science in novel and emerging nanomaterials such as thin films, layered materials and two-dimensional semiconductors. Her work emphasizes optoelectronic properties, device fabrication, and fundamental theories in light-matter interactions.

Xiaolin Wang is a Senior Lecturer at the Australian National University (ANU) and a DECRA Fellow of the Australian Research Council (ARC). She received her PhD in 2017 from ANU. To date, she has secured two million research funding from ARC and the Australian Renewable Energy Agency. She holds 15 patents, three out of which have been commercialised. She was a recipient of several awards such as 2021 ANU Vice-Chancellor's Award for Early Career Academics, 2020 Excellence of HVAC&R Research, and 2016 Research Student of the Year from the Australian Institute of Refrigeration, Air-conditioning and Heating. Shannon is the Sub-Dean of Student Experience and is dedicated to supporting emerging women in STEM and early-career academics.

Dewei Chu is a full Professor in School of Materials Science and Engineering at the University of New South Wales. He received his Ph.D. degree in materials science from the Shanghai Institute of Ceramics, Chinese Academy of Science, in July 2008. He worked at the Advanced Institute of Science and Technology (AIST) Japan for three years. His research group targets to develop solution-processed, printable, and flexible nanoionic materials for cost-effective and energy-efficient wearable electronics.

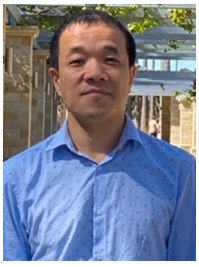

Wenlong Cheng is a Professor in the School of Biomedical Engineering at the University of Sydney and a former director of research at Monash University's Department of Chemical & Biological Engineering. He is an NHMRC Investigator Leadership Fellow, a fellow of the Royal Society of Chemistry, and a former Ambassador Tech Fellow at the Melbourne Centre for Nanofabrication. He founded the Monash NanoBionics lab in 2010, focusing on the Nano-Bio Interface, particularly self-assembly of 2D plasmonic nanomaterials, DNA nanotechnology, electronic skins, and stretchable energy devices. He has published over 200 papers and serves as a scientific editor for Nanoscale Horizon and on the editorial boards of Nanoscale, Nanoscale Horizons, Nanoscale Advances, etc.

Yi Xi is now a Professor at Chongqing University, China. She received her PhD degree in Physics from Chongqing University in 2010. Her main research interests focus on the fields of piezoelectric, triboelectric nanogenerators for energy harvesting and supercapacitors for energy storage, self-powered sensor system. She is the author of more than 150 publications and holds more than 20 patents.

Yuerui Lu is a Professor in the School of Engineering at the Australian National University, and chief investigator and program manager at the Australian Research Council Centre of Excellence for Quantum Computation and Communication Technology. He received his Ph.D. degree from Cornell University in 2012, and B.S. degree from University of Science and Technology of China. He was the recipient of several competitive awards, including the prestigious Malcolm McIntosh Prize for Physical Scientist of the Year in the Prime Minister's Prizes for Science in 2023, and Pawsey Medal from Australian Academy of Science in 2023, etc. His research interests include 2D quantum materials and optoelectronic devices, MEMS sensors and actuators, biomedical devices, etc.